A STUDY OF ROLLING ADHESION IN BRAKING

by

John Roy D'Sa

Thesis submitted to the Graduate Faculty of the
Virginia Polytechnic Institute and State University
in partial fulfillment of the requirements for the degree of
MASTER OF SCIENCE
in
Mechanical Engineering

APPROVED:

R. L. Whitelaw, Chairman

N. S. Eiss

H. H. Mabie

August, 1978

Blacksburg, Virginia

3

ACKNOWLEDGMENTS

The author expresses his deep appreciation to Professor R. L. Whitelaw for his guidance and assistance in the course of his graduate program of study and his thesis work. The analysis of the experimental data and drawing up of conclusions was possible due to the assistance of Dr. N. S. Eiss. The selection and use of proper bearings on the rig was guided by Dr. H. H. Mabie.

He is also grateful to Mr. Martin J. Vann for the design of the test rig and for his work in the instrumentation and the collection of test data.

The author acknowledges the drafting assistance of Ms. Pat Crocker and thanks Mrs. Elizabeth Daws for her excellent typing of this thesis.

Lastly, the author thanks his parents for their love, encouragement and understanding throughout his college career.

TABLE OF CONTENTS

Page

LIST OF FIGURES

List of Tables

NOMENCLATURE

Symbol	Notation
a	semi-major axis of the contact ellipse
A	constant obtained from Hertzian equations
b	semi-minor axis of the contact ellipse
B	constant obtained from Hertzian equations
E	modulus of elasticity
K_1, K_2	material constants used in the Hertzian equations
m, n	constants determined from tables, used in the Hertzian equations
N	normal force at the contact area
R_1, R_1'	principal radii of one body
R_2, R_2'	principal radii of second body
$v_{\text{contact area}}$	velocity into the contact ellipse
V_{A1}	velocity of approach of one body
V_{A2}	velocity of approach of second body
θ	value used to determine m and n from tables for the Hertzian equations
θ_1	angle between the deformed and the undeformed radii at the contact ellipse of one body
θ_2	angle between the deformed and the undeformed radii at the contact ellipse of the second body
ω_1	angular speed of rotation of one body
ω_2	angular speed of rotation of second body

1. INTRODUCTION

It is necessary to define some of the terms used in the literature related to rolling phenomena, before one discusses the scope of this report. This is relevant since various authors have used common terms at cross purposes and as a result there is some confusion in terminology. For the purposes of this report the following definitions will be used:

a) Rolling resistance: The tangential force acting at the contact surface of one body rolling on another, solely due to rolling.

b) Tractive force: The tangential force transmitted at the contact surface by a forward torque applied to one rolling body.

c) Friction coefficient: The ratio of the tangential force to the normal force in pure sliding motion.

d) Adhesion coefficient: The ratio of the tangential force to the normal force when one rolling body slips relative to the other.

e) Contact velocity: The velocity of approach into the contact area given by the magnitude of the smaller semi-axis of the ellipse of contact times the angular velocity.

In the past few years there has been a very keen interest in the phenomenon of rolling adhesion. The study and research has been possible partly because of a fillip given in recent years by industry and also to a large measure due to the own interests of the researchers involved. A brief list of engineering situations to which rolling adhesion has been applied is the rolling motion of wheels of various types, ball and roller bearing design,

gear teeth where the motion is a combination of rolling and sliding, variable speed friction drives and others.

Engineers and researchers involved in the wheel-rail adhesion of locomotive wheels have in the past investigated means of improving the tractive efficiency of locomotives. Studies were directed at the investigation of the effects of contaminants on rails, the study of the variation of the coefficient of adhesion with speed, rail shape, and rail wear. Very little is known of the interdependence of load and velocity, if any, in the contact area of two rolling bodies.

The availability of a test rig to simulate locomotive wheel-on-rail action at the mechanical engineering department of the Virginia Polytechnic Institute and State University provided an opportunity to study the effect of load and velocity into the contact area. In previous work on the test rig, the variation of the coefficient of adhesion with speed was studied and an algebraic relation predicting this variation with speed postulated.

This thesis presents the results of separating out the effects of load and velocity in the contact area, which in the present case is an ellipse, of one wheel rolling on another larger wheel. A review of the literature available concerning rolling motion is presented. A description of the test rig and testing procedure is included. The results and conclusions follow with recommendations for the scope of future research.

2. LITERATURE REVIEW

There has been a considerable amount of experimental research and theoretical work in the field of rolling adhesion both in this country and in England. It would be inappropriate for this report to offer a comprehensive review of the vast amount of literature available on the rolling adhesion phenomena and its related questions. However past investigations and theories which have a bearing on the present work will be discussed.

Various theories have been proposed concerning the mechanics of rolling motion. A recent theory proposed by K. Kendall (1) in 1975 explains rolling friction viz., the resistance that one free rolling body faces when it rolls on another, in terms of crack propagation through an adhesive joint. The contact between a smooth cylinder and flat surface has been regarded as an adhesive junction bounded by two cracks moving in the same direction at the same speed, one crack continually opening and the other continually closing. Propagation of these cracks requires a force which is calculated on the basis of crack theory and shown to be equal to the observed rolling friction.

The theory was verified experimentally using glass cylinders rolling on smooth rubber. The positive features of this theory are that it successfully predicts a static rolling friction and also the effect of a lubricant or dust.

Break surface energy, viz. the energy required to break the covalent bonds formed between rubber and glass, is used to predict the

drop in rolling friction at high rolling speeds. The increase in break surface energy is due to an increased dwell time of rubber on glass i.e., an increased time of contact. Figure 1 shows a plot of the data on which the drop in rolling friction was explained. An extension of this argument would imply that rolling friction is time dependent.

N. A. Greenwood and D. Tabor (2) in 1958 attributed rolling friction to elastic hysteresis losses supposedly occurring when the contact surface is first stressed and then the stress released as rolling continues and the point of contact moves on. The observed energy losses in rolling conformed with the predicted values from the hysteresis model and were fairly supportive of the model. However, the hysteresis loss factor was assumed constant thereby suggesting that it was independent of the strain rate. This would indicate that the free rolling resistance is independent of velocity.

D. Tabor (3) in 1956 suggested that pure rolling conditions would prevail if the contact of two bodies were a point. In practice, however, the region of contact is elastically deformed so that contact is made over an area of some size, the points within it lying in different planes as shown in Fig. 2. In consequence, it is not possible for pure rolling action to take place except at a very small number of points, but rather, at all other points there is a combination of rolling and a small degree of slip. To achieve this slipping requires that sliding resistance at the interface be overcome and to accomplish this it is necessary that a rolling friction force act. It is however doubtful

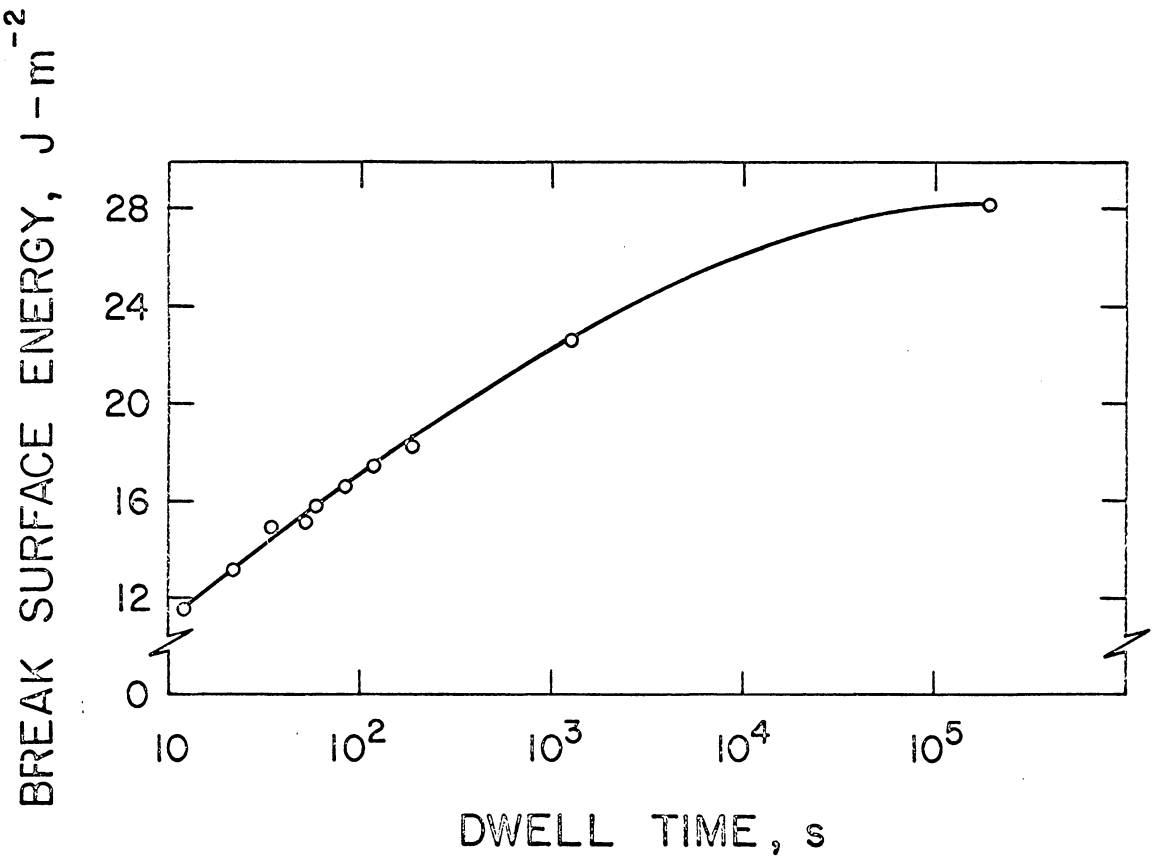

Fig. 1. Variation in break surface energy with dwell time of rubber on glass (from Kendall (1), Fig. 5)

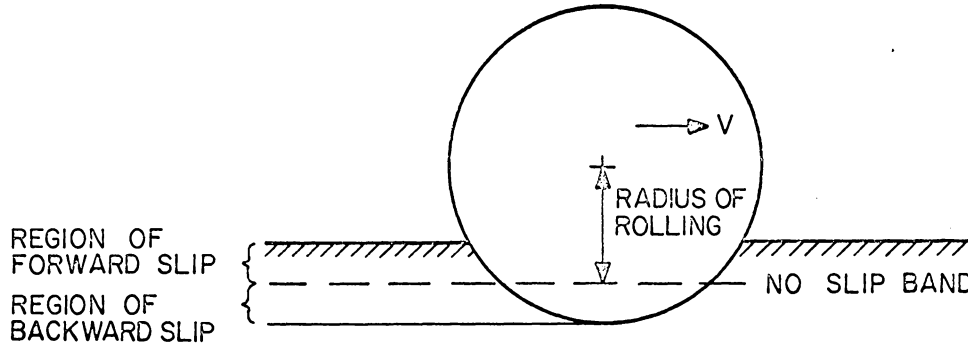

Fig. 2. A sphere rolling on a flat surface (from Rabinowicz (12), Fig. 4.30)

whether slip velocities which are generally small, usually 5% or less of the overall rolling velocity according to Tabor, can produce a major portion of the total resistance to rolling. On the other hand in some cases the surfaces tend to spin about the region of contact or there may be gross slippage as a result of which the contribution of slip to rolling friction would be significant.

Having thus reviewed some of the theories of rolling friction, it would be pertinent at this point to comment that while there is no broad consensus on these theories, there is in comparison greater agreement on the theories of tangential stress distribution, a typical example of which is the K. L. Johnson's theory.

K. L. Johnson (4) in 1960 studied the motion and deformation of an elastic sphere rolling on an elastic plane, under a normal contact pressure for the case where the point of contact also sustained a tangential force. The study was based to a large extent on a paper presented by F. W. Carter in 1926 in which he derived the tangential stress distribution over the contact area between a locomotive wheel and rail. When the sphere rolled without sliding it exhibited a small velocity relative to the plane called "creep". K. L. Johnson showed that creep arose from a part of the area of contact and that further this slip took place towards the trailing edge of the contact area. He assumed a locked region in which no slip occurred to be of circular shape and that it was tangential to the circle of contact at its leading point. There is however no theoretical or experimental basis to support this assumption. Based on this assumption, he predicted the surface tractions which satisfy the

conditions of no slip within the locked region and which were approximately consistent with the laws of friction in the slip region. Experimental measurements of a steel ball rolling on a flat steel surface were in fair agreement with the theoretical results.

Despite the large amount of literature available on rolling adhesion, actual experimental research in rolling adhesion by simulation of locomotive wheel on rail or actual test of locomotive wheels on rails is rather limited as most research deals with simple rolling experiments. M. J. Andrews (5) in 1958 studied the interaction of a locomotive wheel on rail. He first experimentally verified whether Hertzian contact considerations were valid for locomotive wheel on rail surface interactions. He found that the experimental results corresponded to the theoretical predictions from Hertzian equations. Later he conducted experiments to verify the effect of load on the "coefficient of friction" at slip. In present terminology what Andrews calls the "coefficient of friction" should be called the coefficient of adhesion. However, the experiments were conducted in the speed range of 0-16 km.p.h. (0-10 m.p.h.), though experiments to verify the coefficient of adhesion at different speeds were conducted in the speed range 0-48 km.p.h. (0-30 m.p.h.). The reduction in the coefficient of adhesion with increasing speed was explained on the basis of increased vibration in the contact zone which increased with speed. He conducted his tests using a powered locomotive which hauled another locomotive, the purpose being to maintain constant speed during each test. The train was run at different

speeds and the tractive force gradually increased to produce slip. Slip was indicated using a differential slip indicator between the axles of the powered and the free locomotive.

L. O. Hewko, R. L. Scott, et al. (6) in 1962 conducted experiments to study the effect on traction and efficiency of such operating variables as rolling contact velocity, normal load, temperature, lubricants, and the geometry of rolling components. The results indicated that while the effects of some of these variables was insignificant, others such as contact velocity, type of lubricant, and surface geometry could produce very large changes in tractive capacity and efficiency. The combined effects of normal load and contact velocity on the coefficient of adhesion at slip are illustrated in Fig. 3 and Fig. 4. Figure 3 shows that as the normal load increases the coefficient of adhesion also increases and peaks in the 4540-6810 kg load (10,000-15,000 lb) region for all speeds. Beyond that load there is a slight, steady decrease in the coefficient of adhesion at higher speeds. The speed effect is considerably greater than the load effect particularly in the low speed region. This is shown more clearly in Fig. 4 which shows the same data as a function of speed. At low contact velocities the drop in traction is very rapid but at higher speeds it tends to reach a constant value. However the research made no attempt to simulate locomotive wheel on rail action and in general had no bearing with the parameters affecting a wheel on rail interaction.

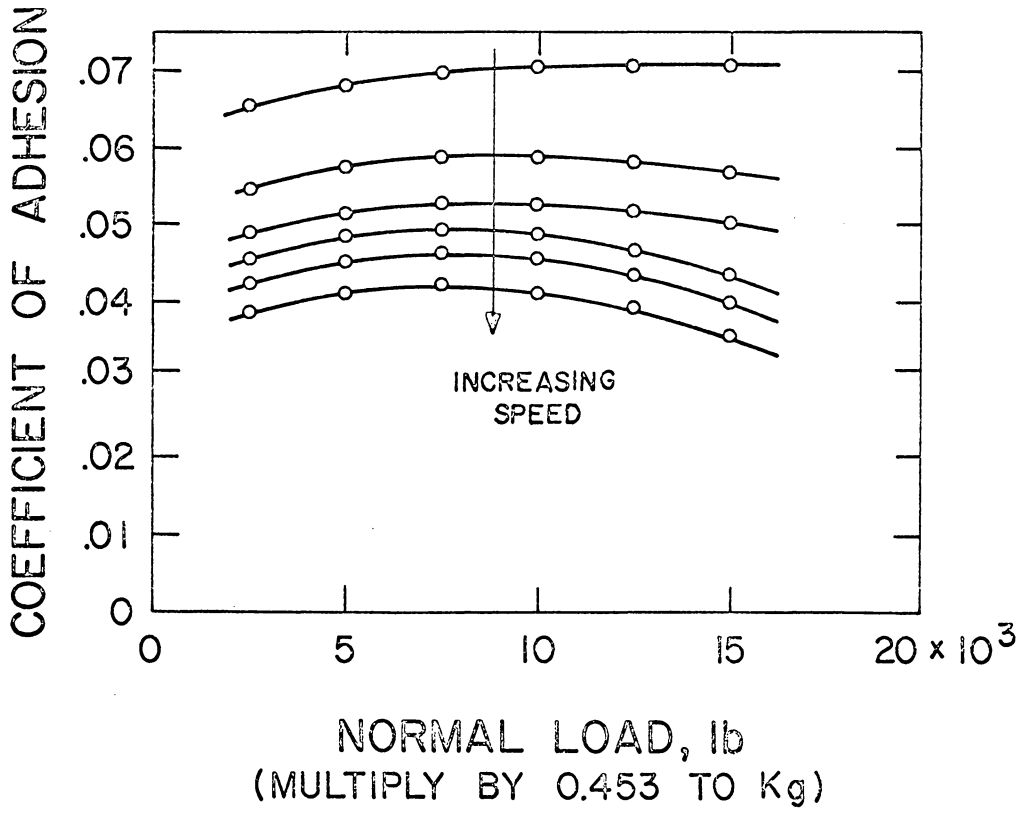

Fig. 3. Effect of normal load on the coefficient of adhesion at different speeds (from Hewko (6), Fig. 7)

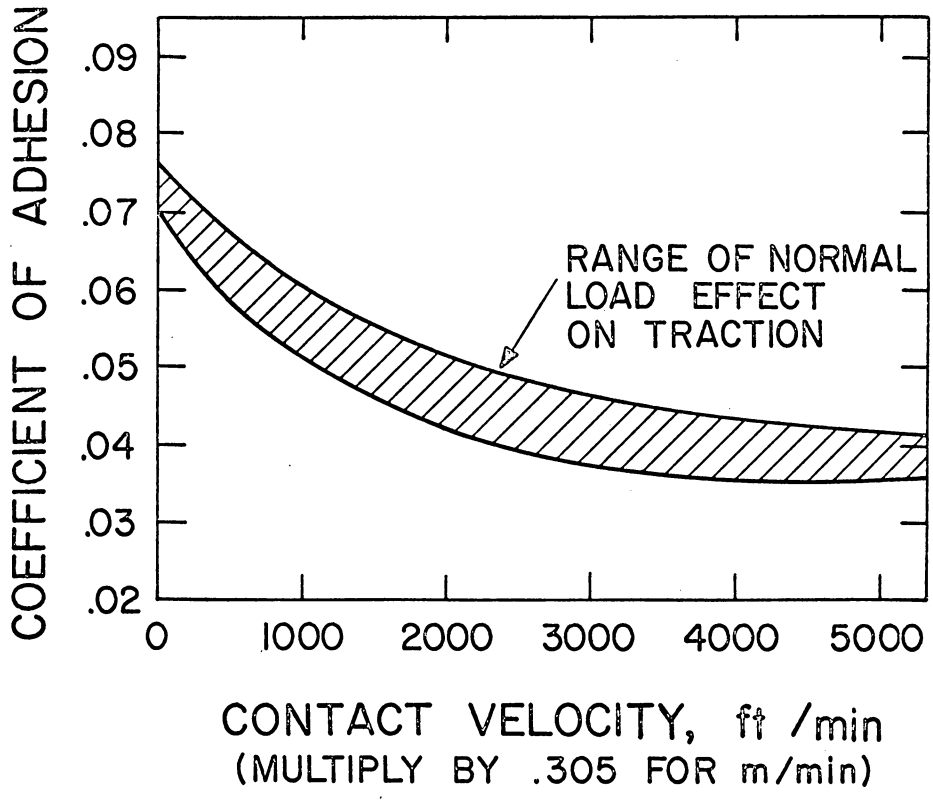

Fig. 4. Effect of contact velocity on the coefficient of adhesion (from Hewko (6), Fig. 8)

J. Koffman (7) in 1948 reviewed most of the literature available pertaining to the variation in the coefficient of adhesion with speed. Table 1 illustrates several relationships proposed by various authors. Koffman concludes that while all the relationships indicate a trend, the specific constants obtained in each case depended on the nature of the experimental tests and the accuracy of the instrumentation.

M. Anderson (8) in 1977 verified the variation in the coefficient of rolling adhesion with surface speed and proposed the relationship, $\mu = (32.81/V) - 0.119$, where V is in km.p.h. The relationship is in fair agreement up to 100 km.p.h. with the investigations of past researchers as examined by Koffman (7).

W. B. Kirk (9) in 1965 studied the efficiencies of various braking systems which were used in high speed train operation. The braking systems studied were an air-brake system, a pneumatic brake system, and a composition brake shoe system. The paper however does not describe or refer to the experimental apparatus used in the tests. Of particular interest to this study are the adhesion coefficient curves shown in Fig. 5 for varying surface speeds. The study showed a very significant drop in the adhesion coefficient when the tests were performed on a wet rail. However the absolute values of the adhesion coefficient obtained by Kirk are open to question since they are not in good agreement with the relationships examined by Koffman (7).

No.	Author	Equation
1	Bochet	$\mu = \frac{0.31}{1 + 0.03V}$
2	Dobrovolsky	$\mu = 0.22 - 0.0012V$
3	Quirchmeyer	$\mu = 250 - 1.4\left(\frac{V}{10}\right)^2$
4	Meineke	$\mu = 250 - 1.5\left(\frac{V}{10}\right)^2$
5	Parodi	$\mu = \frac{0.22}{1 + 0.01V}$
6	Babichkov	$\mu = \frac{1}{3.2 + 0.035V}$
7	Curtius	$\mu = \frac{7500}{V + 44} + 161$
8	Karvatzki	$\mu = 0.24 - 0.0007V$
9	Kother	$\mu = \frac{9000}{V + 42} + 116$

Table 1. Equations proposed by various authors to predict the variation of the coefficient of adhesion with speed, V - km.p.h. (from Koffman (7), Table 1)

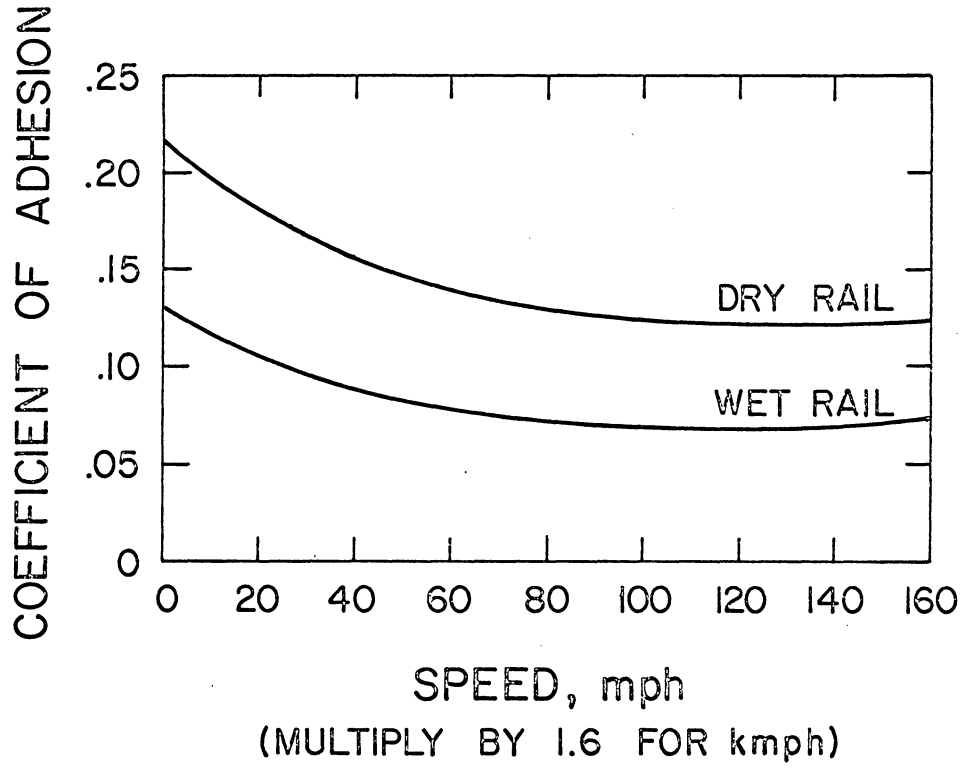

Fig. 5. Adhesion coefficients for wet and dry rails (from Kirk (9), Fig. 6)

J. T. Burwell and E. Rabinowicz (10) in 1953 conducted experiments which proved that the friction force is a function of normal load and the sliding speed. They concluded that speed can influence the friction force in two ways -- one by the resulting shear strain rate in the vicinity of the welded junction and the other by the length of time taken for a junction of full strength to form. Figures 6 and 7 indicate the coefficient of friction as a function of final sliding velocity for two cases viz., steel on indium and steel on lead respectively. The experimental apparatus consisted of a brass block into one surface of which had been screwed three steel, hemispherically ended sliders which rested on a clean, flat horizontal surface consisting of indium on lead. The tangential force was applied by a load and pulley arrangement, the point of application of the force being about 25.4 mm (1.0 in.) above the horizontal surface. The displacement was measured by observations of the movement of a scratch in the upper surface of the brass block in relation to a scale fixed with respect to the bottom surface. The rise and subsequent fall of the coefficient of friction with increasing speed is explained on the basis of the primary and secondary phases of creep. Since it takes a finite time for a weld when formed to reach its full strength, at increased speeds this weakening of the weld outweighs the increased force required by the increased strain rate.

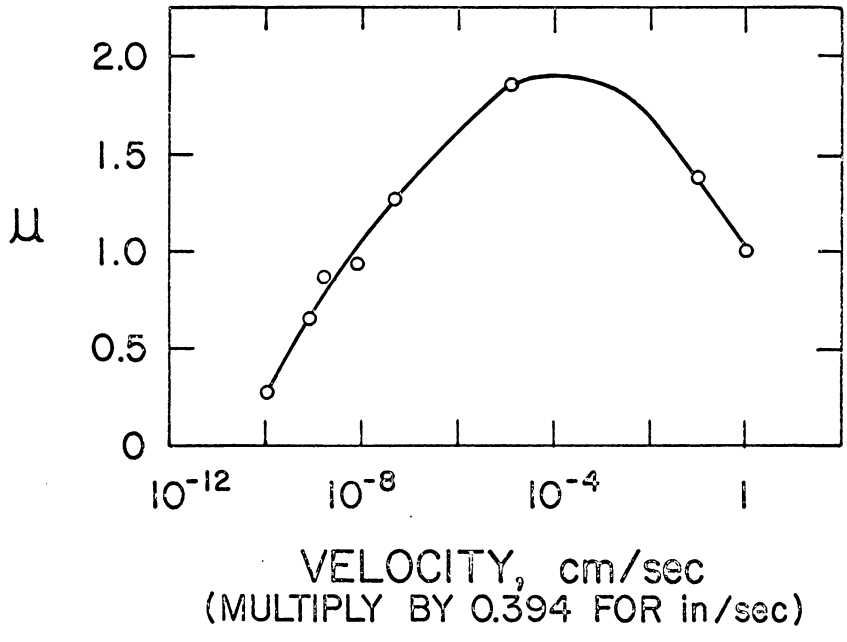

Fig. 6. Coefficient of friction as a function of final sliding velocity. Steel on indium (from Rabinowicz (10), Fig. 4)

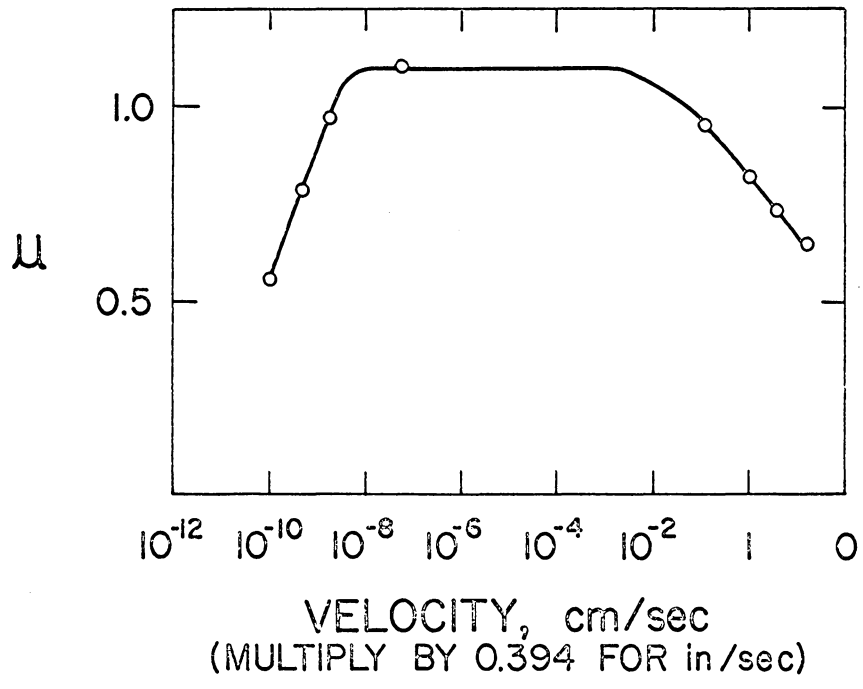

Fig. 7. Coefficient of friction as a function of final sliding velocity. Steel on lead (from Rabinowicz (10), Fig. 5)

3. EXPERIMENTAL APPARATUS AND PROCEDURE

3.1 Description of Test Rig

The test rig used in the work described in this report is sketched in Fig. 8, 9, and 10 and pictured in Fig. 11, 12 and 13. The test rig consists of a 7.5 KW d.c. motor A which drives a 58.42 cm (23.0 in.) diameter wheel B made of cast steel, which is referred to as the large wheel. On either side of the large wheel B and in contact with it -- during the experimental tests -- are two 5.08 cm (2.0 in.) diameter wheels C referred to as small wheels. The small wheels C and the large wheel B simulate the locomotive wheel-on-rail action and would be analogous to the locomotive wheel and the rail, respectively. The purpose of using two small wheels is to detect the incidence of slip by instantaneous comparison of their speeds. The small wheel which is braked (or overdriven) to force it to slip relative the large wheel B is mounted on a shaft which on the one side can be coupled (through a flexible coupling) to a 0.25 KW a.c. motor D and which is on the other side integral with the aluminum disk E of the eddy current brake F. The motor D was used to overdrive the small wheel to measure the coefficient of adhesion in acceleration, in a separate investigation conducted by Martin J. Vann for his Master of Science thesis.

The electromagnets of the eddy current brake, the shaft bearing supports and the motor D are attached or mounted on the load

arm G which is pivoted at one end through a univeral joint S. The purpose of the load arm is threefold:

1. To serve as a support for the shaft bearing supports.
2. To act as a means of applying normal force at the small wheel/large wheel interface.
3. To serve as a means of torque measurement.

The values of the torque and normal force are necessary to evaluate the coefficient of adhesion at slip.

The load arm consists of an U-channel at the end of which, the torque tube H is mounted. The torque tube which consists of strain gages mounted on a hollow tube is used to measure the torque applied by the eddy current brake at the instant of slip.

The load is applied by placing 1 kg (2.2 lb) masses on the load pan I that is connected through the nylon cable J to the load arm extension K. The load pan is free to move on the wire cable due to pulley L thus maintaining a constant load on both the arms. Pulley M directs the vertical load into a horizontal force.

The load arm extension K passes through the torque tube H and is attached on to the load arm G. One end of the torque tube is mounted on the load arm G while the other end is mounted on the yoke N.

The universal joint serves to:

1. Adjust the vertical position of the load arm.
2. Allow for lateral, in and out movement of the load arm.

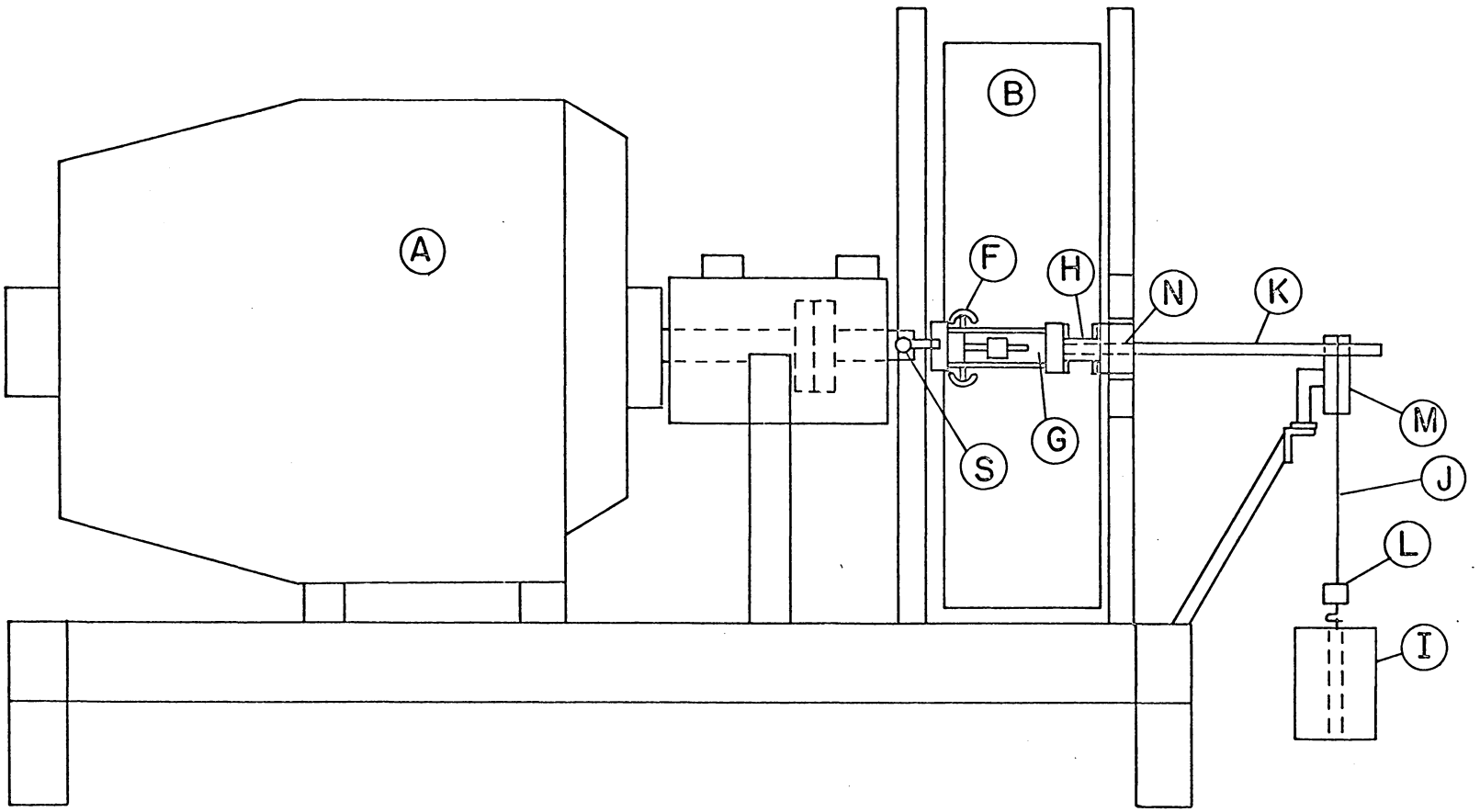

Fig. 8. Side view of the test rig. A-D. C. Motor, B-Large Wheel, F-Eddy Current Brake, G-Load Arm, H-Torque Tube, I-Load Pan, J-Nylon Cable, K-Load Arm Extension, L, M-Pulleys, S-Universal Joint

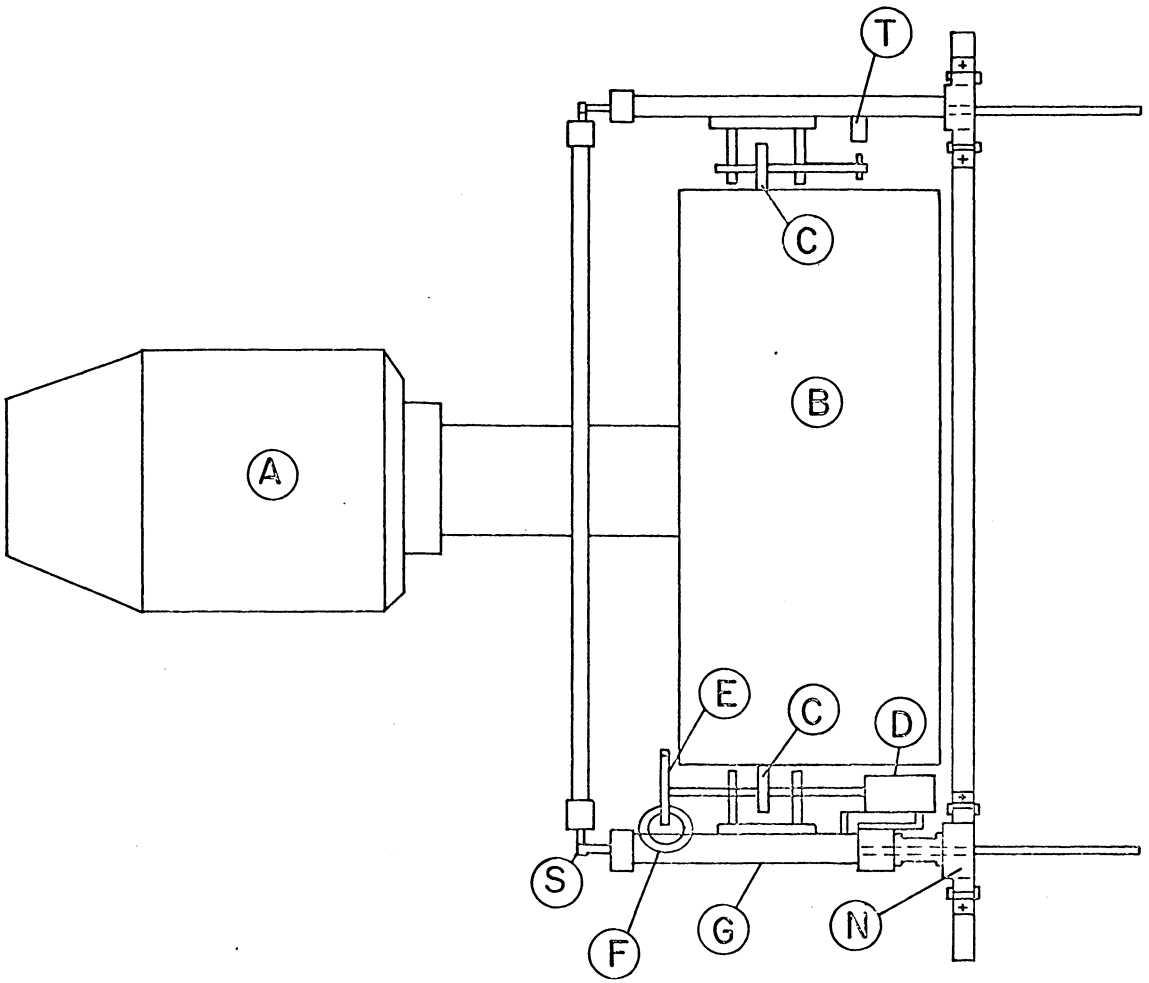

Fig. 9. Plan view of the test rig. A-D. C. Motor, B-Large Wheel, C-Small Wheel, D-A. C. Motor, E-Aluminum Disk, F-Eddy Current Brake, G-Load Arm, S-Universal Joint , T-Transducer

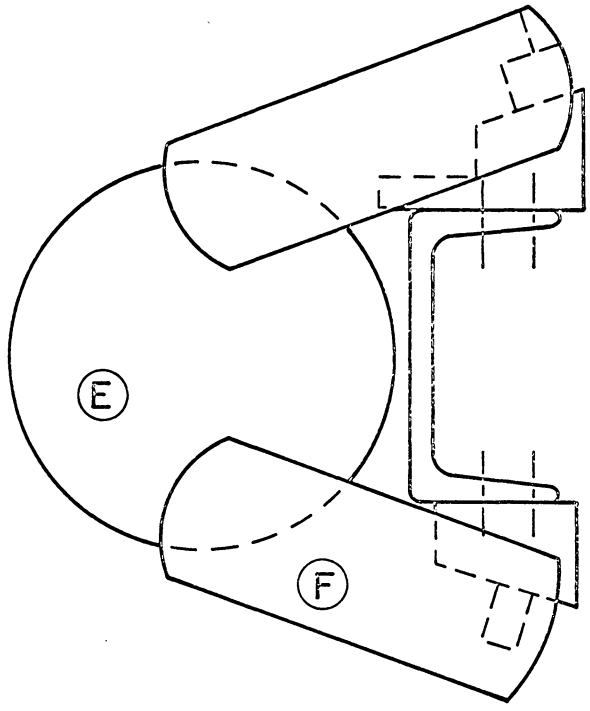

Fig. 10. Side elevation showing eddy current brake mounting
E-Aluminum Disk, F-Eddy Current Brake Pole Piece

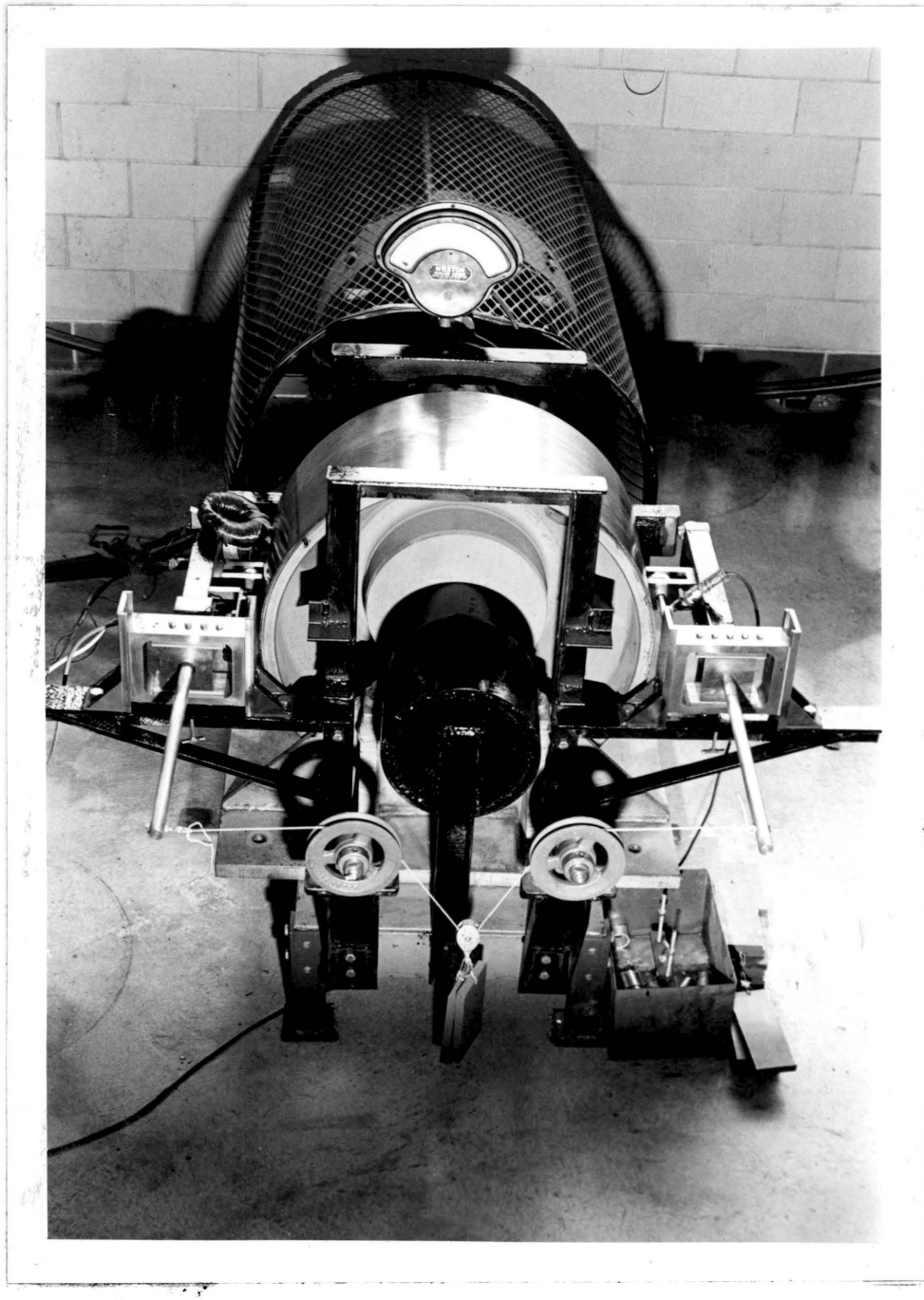

Fig. 11. Experimental test rig (front view)

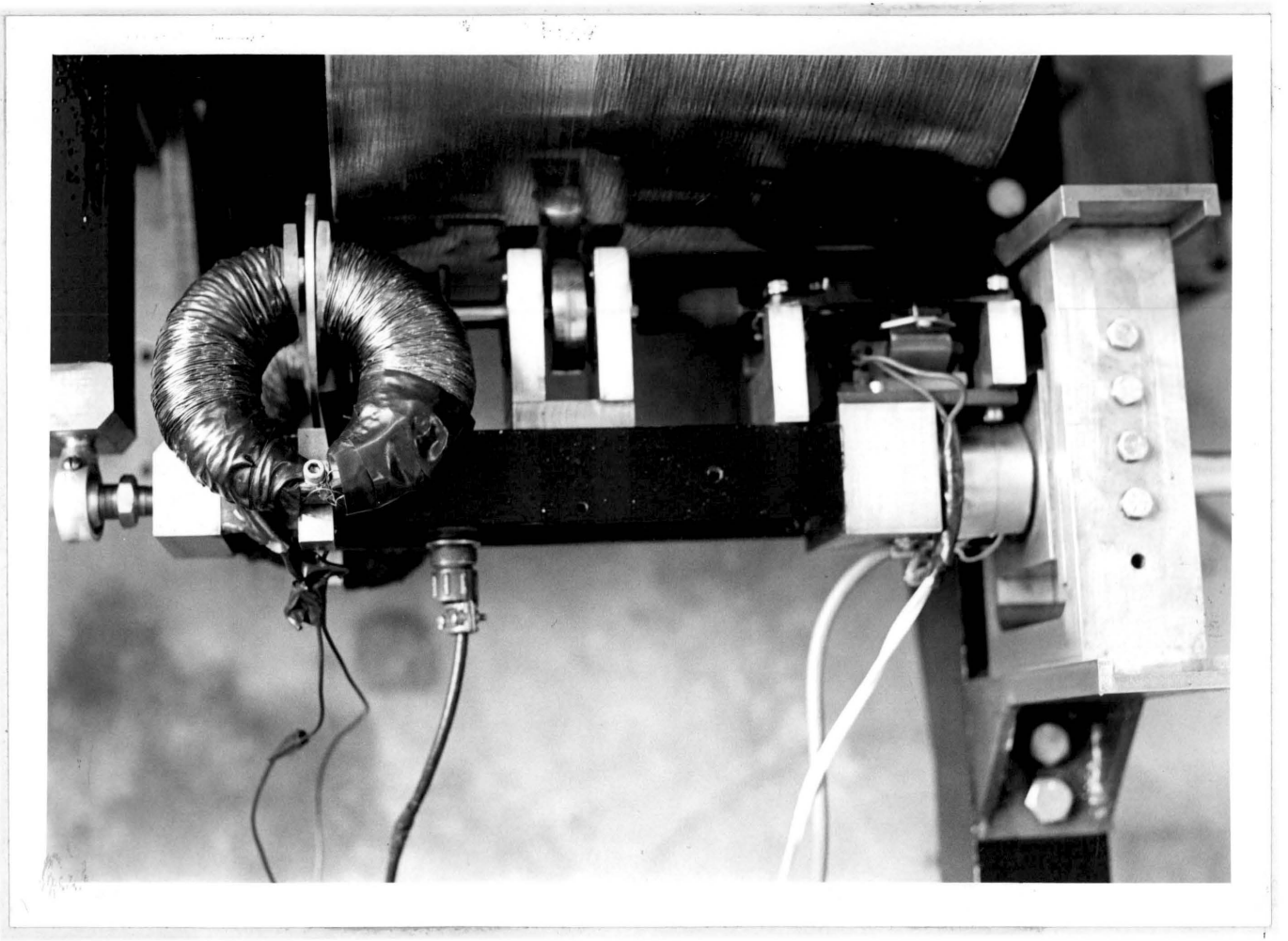

Fig. 12. Experimental test rig (close-up of brake)

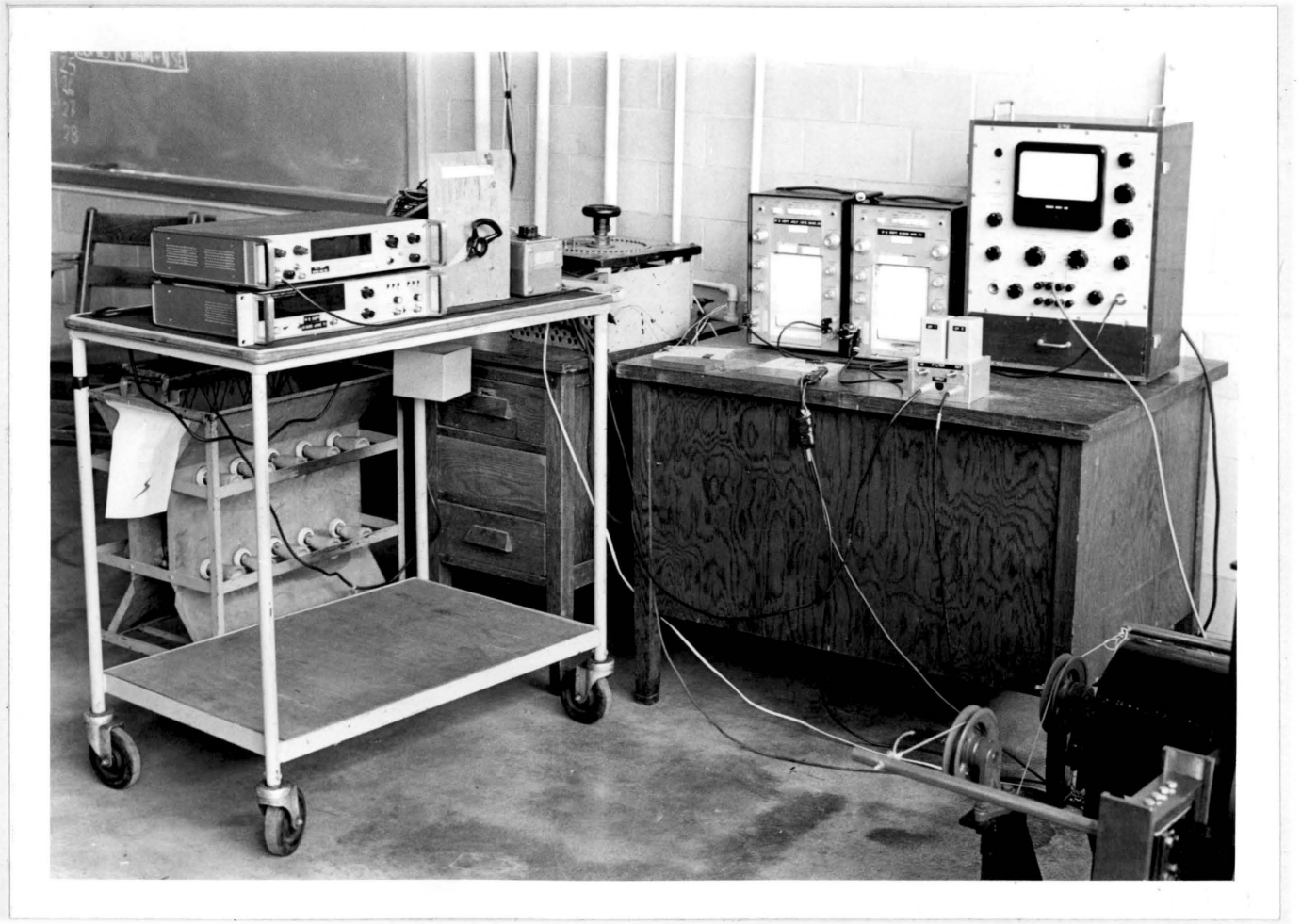

Fig. 13. Experimental test rig (instrumentation)

The friction due to this lateral movement at the yoke N is minimized through use of teflon coated metal plates.

The speed into the contact area can be varied by changing the rotational speed of the D.C. motor through control of the armature field current.

3.2 Instrumentation

A block diagram of the instrumentation set-up is shown in Fig. 14. Magnetic transducers were used to sense the rotational speeds of both the reference wheel and the braked wheel. The transducers received input signals from screws which were fixed on shafts carrying the small wheels. The transducers were connected on to Hewlett-Packard frequency counters which were used for speed calibration. Since a double ended screw was used, the frequency displayed on the counter was twice the actual frequency of rotation of the shaft. However since the time lag between successive readings of the frequency counter is of the order of seconds and not of the order of milliseconds as would be required for the purposes of the testing, visual use of the Hewlett-Packard frequency counter as a means of speed comparison to detect slip was unsuitable for the purposes of the test.

The output of the magnetic transducer is in the form of an a.c. signal (around 8 volts r.m.s.) and hence could not be fed directly into the Brush Mark II strip chart recorder. As a result a full wave bridge rectifier-filter circuit had to be used to rectify the output signal from the magnetic transducer. The rectified

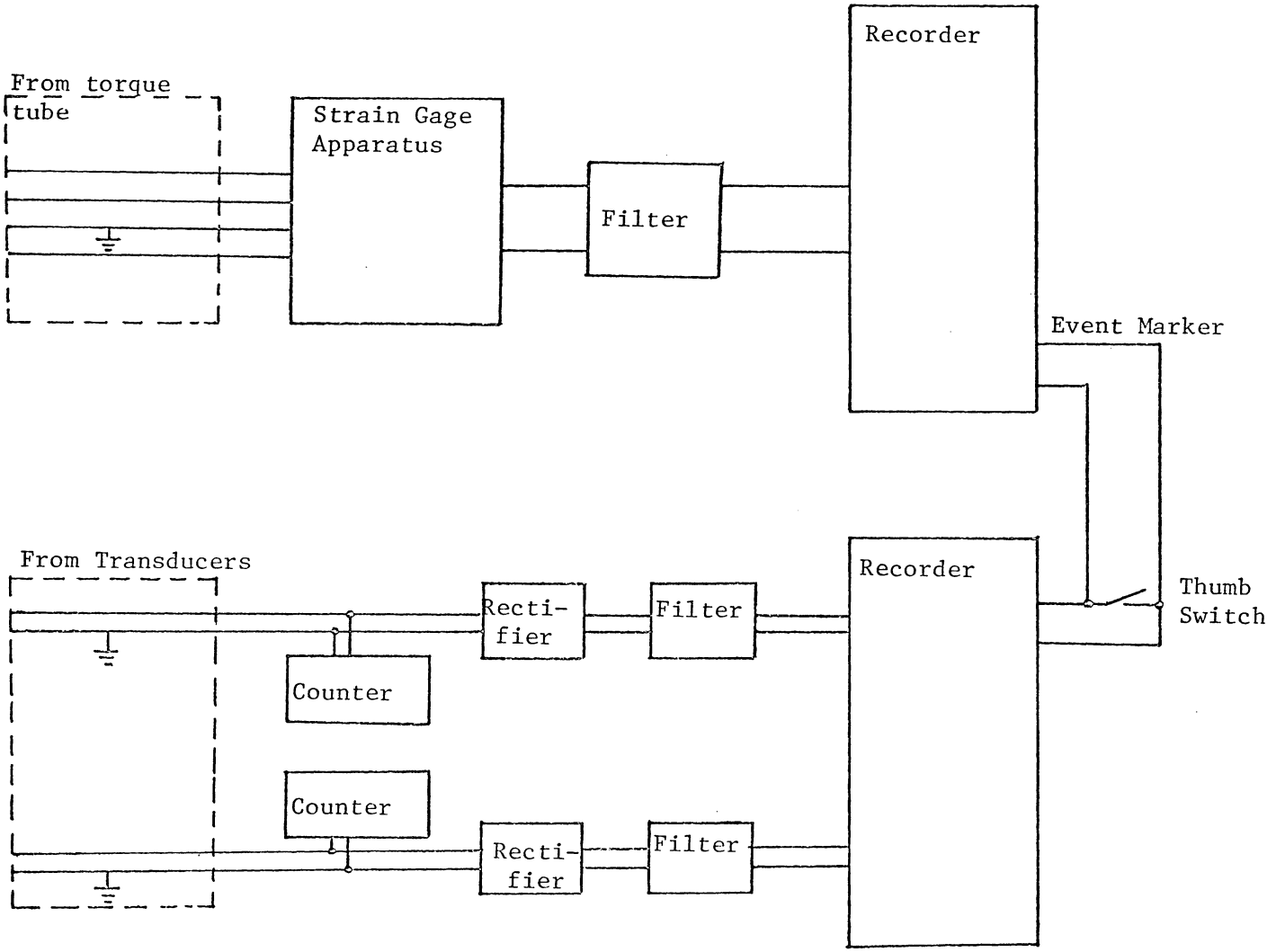

Fig. 14. Block diagram of instrumentation set-up

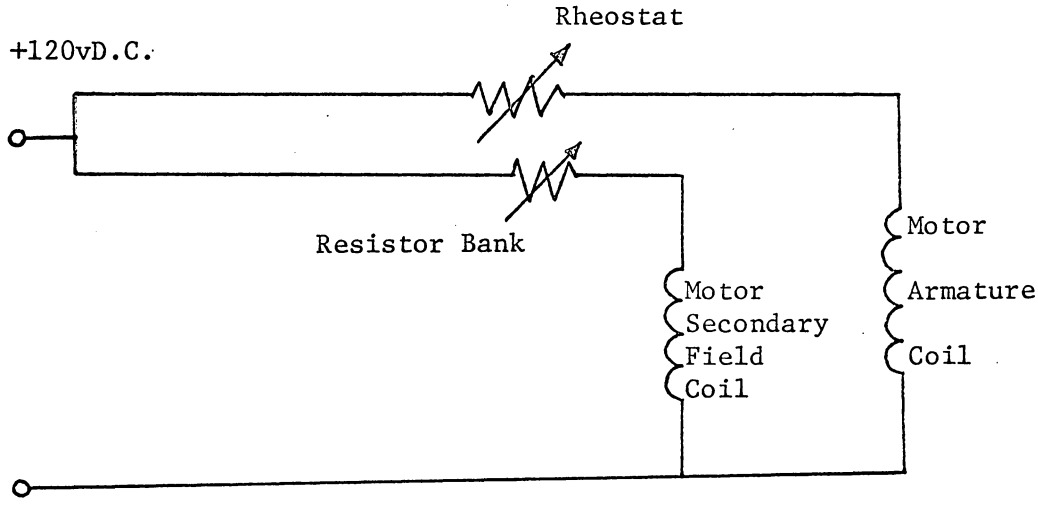

Fig. 15. Control circuit of d. c. motor

signal supplied to the strip chart recorder served to detect the onset of slip when the signal from the channel connected to the transducer of the braked wheel fell away from the signal of the unretarded wheel. The magnetic transducers were mounted on the load arms -- on the braked wheel side the transducer was screwed on directly on to the side of the channel section, whereas on the reference wheel side the transducer was mounted on a specially designed mounting bracket. The output signals of the transducers were matched on a cathode ray oscilloscope and equalised by either threading the transducers in or out with respect to the screwheads from which the transducers received their signals.

An eddy current torque brake was used to force the small wheel to slip with respect to the large wheel. The torque at slip was measured using a torque tube, a Breul and Kjaer strain gage apparatus, and a Brush Mark II strip-chart recorder. The strain gages of the torque tube were connected to the strain gage apparatus whose output was fed into the strip chart recorder through a resistance-capacitance filter. The torque tube consists of four-arm strain gages cemented to two flat spots on a hollow steel tube. The torque tube was designed to measure a minimum strain of 50 μin./in. which was well sufficient for the purposes of this test. However, due to the increased sensitivity, of the torque tube the strain gages picked up the vibrations of the test rig and of the load arm and which were obviously undesirable for accurate measurements of torque at slip. A resistance-capacitance filter was used to cut

out the signals caused by the vibrations of the test rig. The filter in effect cut out the waviness of the output torque signal on the strip chart recorder. However the values of the resistance (1000 ohms) and capacitance (15 microfarads) were selected such that the response of the system was not unduly affected.

It was also observed that the magnetic field of the Variac of the eddy current brake affected the readings of the strain gages. This error was rectified by placing the Variac as far away from the strain gages as possible and also by shielding the strain gages using an aluminum foil. The strip chart recorder was operated at 125 mm/sec.

A thumb switch operating the event markers of both the strip chart recorders was used to correlate the exact instances at which the tests were started.

3.3 Test Procedure and Log of Tests Conducted

The experiments were conducted in the fluid mechanics laboratory with an average humidity at 80 RM and temperature at $30^{o}C$ ($80^{o}F$). For a particular speed of the small wheel, readings were taken with 1.0, 2.0, 3.0, 4.0, 5.0 kg masses in the load pan. Subsequently by adjusting the voltage across the secondary field coil and for the armature coil of the large D.C. motor, the speed of the small wheel was raised to a predetermined level and the experimental procedure outlined above repeated for different loads.

Speed calibration was done by use of the 'sensitivity' and 'position' controls on the Brush strip chart recorder.

To obviate any bending strains introduced at the torque tube due to bending of the load arm, torque calibration was done at the small wheel itself. Known weights were attached to a lever which was screwed on to the load arm and the calibration torque recorded on the strip chart recorder. The torque calibration was performed with the large wheel running, this done to cancel out any superimposed signals due to vibrations of the torque tube. A calibration curve of torque versus the number of division on the strip chart recorder was then plotted.

Table 2 indicates a log of the readings taken at various loads and speeds.

Table 2. Log of readings at various loads and speeds.

Rotational speed of small wheel (rpm)	Number of 1.0 kg (2.2 lbm) masses in load pan				
	1	2	3	4	5
5770	X	X	X	X	X
6490	X	X	X	X	X
7270	X	X	X	X	X
8310	X	X	X	X	X
8180	X				
9310	X				
9870	X				
10350	X				
11100	X				
11560	X				
11960	X				
12430	X				
13215	X				
14210	X				

4. RESULTS

Initially test readings for the coefficient of adhesion at slip were taken at four different speeds (of 5770, 6490, 7270 and 8310 rpm) of the small wheel and 5 different masses in the load pan - 1.0, 2.0, 3.0, 4.0, 5.0 kg respectively. Subsequent readings were taken for a constant mass of 1.0 kg in the load pan and different speeds -- the speeds selected based on calculations shown in Appendix 9.2. To ensure sufficient accuracy each test reading was repeated three times.

It is important to add that given the nature and characteristics of the speed control of the large D.C. motor, speed control to preselected speeds was achieved to within an accuracy of ±5.0%. Also for the cases of calculated speeds of the small wheel where the differences were not significant, test readings for one representative speed were taken. There were two such instances. For calculated speeds of 9160, 9350 rpm and 10320, 10470 rpm, test readings at speeds of 9310 and 10350 rpm were taken.

Table 3-8 indicate the coefficient of adhesion values obtained for the different speeds and loads for which the tests were conducted.

Table 3. Values of the coefficient of adhesion obtained for a speed of rotation of 5770 rpm of the small wheel

	Number of masses in the load pan				
	1	2	3	4	5
Coefficient of adhesion μ	0.282	0.291	0.250	0.295	0.306
	0.310	0.294	0.270	0.276	0.293
	0.283	0.321	0.284	0.275	0.281
$\mu_{average}$	0.291	0.302	0.268	0.282	0.293
95% confidence limit	0.032	0.033	0.034	0.023	0.035

Table 4. Values of the coefficient of adhesion obtained for a speed of rotation of 6490 rpm of the small wheel.

	Number of masses in the load pan				
	1	2	3	4	5
Coefficient of adhesion μ	0.250	0.221	0.246	0.261	0.234
	0.235	0.196	0.223	0.242	0.248
	0.222	0.204	0.245	0.250	0.263
$\mu_{average}$	0.236	0.207	0.238	0.251	0.248
95% confidence limit	0.028	0.026	0.026	0.019	0.041

Table 5. Values of the coefficient of adhesion obtained for a speed of rotation of 7270 rpm of the small wheel

	Number of masses in the load pan				
	1	2	3	4	5
Coefficient of adhesion μ	0.222	0.230	0.208	0.221	0.160
	0.215	0.206	0.214	0.187	0.172
	0.211	0.194	0.233	0.189	0.193
$\mu_{average}$	0.216	0.210	0.218	0.198	0.175
95% confidence limit	0.011	0.039	0.026	0.038	0.033

Table 6. Values of the coefficient of adhesion obtained for a speed of rotation of 8310 rpm of the small wheel

	Number of masses in the load pan				
	1	2	3	4	5
Coefficient of adhesion μ	0.183	0.149	0.169	0.160	0.141
	0.145	0.138	0.172	0.143	0.117
	0.140	0.132	0.145	0.166	0.119
$\mu_{average}$	0.156	0.140	0.162	0.156	0.125
95% confidence limit	0.047	0.018	0.032	0.024	0.027

Table 7. Values of the coefficient of adhesion obtained for a mass of 1.0 kg (2.2 lb) in the load pan and different rotational speeds of the small wheel.

	Rotational speed of the small wheel, rpm				
	8180	9310	9870	10350	11100
Coefficient of adhesion μ	0.170	0.190	0.146	0.116	0.101
	0.174	0.173	0.122	0.095	0.090
	0.151	0.163	0.152	0.098	0.092
$\mu_{average}$	0.165	0.175	0.140	0.103	0.094
95% confidence limit	0.025	0.027	0.032	0.023	0.012

Table 8. Values of the coefficient of adhesion obtained for a mass of 1.0 kg (2.2 lb) in the load pan and different rotational speeds of the small wheel.

	Rotational speed of the small wheel, rpm				
	11560	11960	12430	13215	14210
Coefficient of adhesion μ	0.095	0.093	0.075	0.050	0.072
	0.074	0.083	0.079	0.057	0.033
	0.083	0.059	0.060	0.014	0.030
$\mu_{average}$	0.084	0.078	0.071	0.040	0.045
95% confidence limit	0.021	0.035	0.020	0.032	0.028

5. DISCUSSION OF RESULTS

The thrust of this thesis work has been to study the interdependence, if any, of load, contact velocity and time of contact in the contact ellipse and thus the experimental results obtained will be analysed in that light.

5.1 Effect of Load and Rolling Velocity on the Coefficient of Adhesion

Figure 16 shows a plot of the coefficient of adhesion against the normal load and the rotational speed of the small wheel.

The plot clearly indicates the absence of any effect of normal load on the coefficient of adhesion. For a fixed speed of rotation of the small wheel on the y axis, there is absolutely no pattern in the variation of the coefficient of adhesion with increasing load. From this we conclude that the normal load has no effect on the coefficient of adhesion. For a fixed normal load and an increasing speed of rotation of the small wheel, the trend for the various normal loads for which tests were conducted indicates a drop in the coefficient of adhesion with increasing speed.

5.2 Effect of "Contact Velocity" on the Coefficient of Adhesion

The coefficient of adhesion was plotted against the velocity into the contact area for the four base speeds of 5770, 6490, 7270

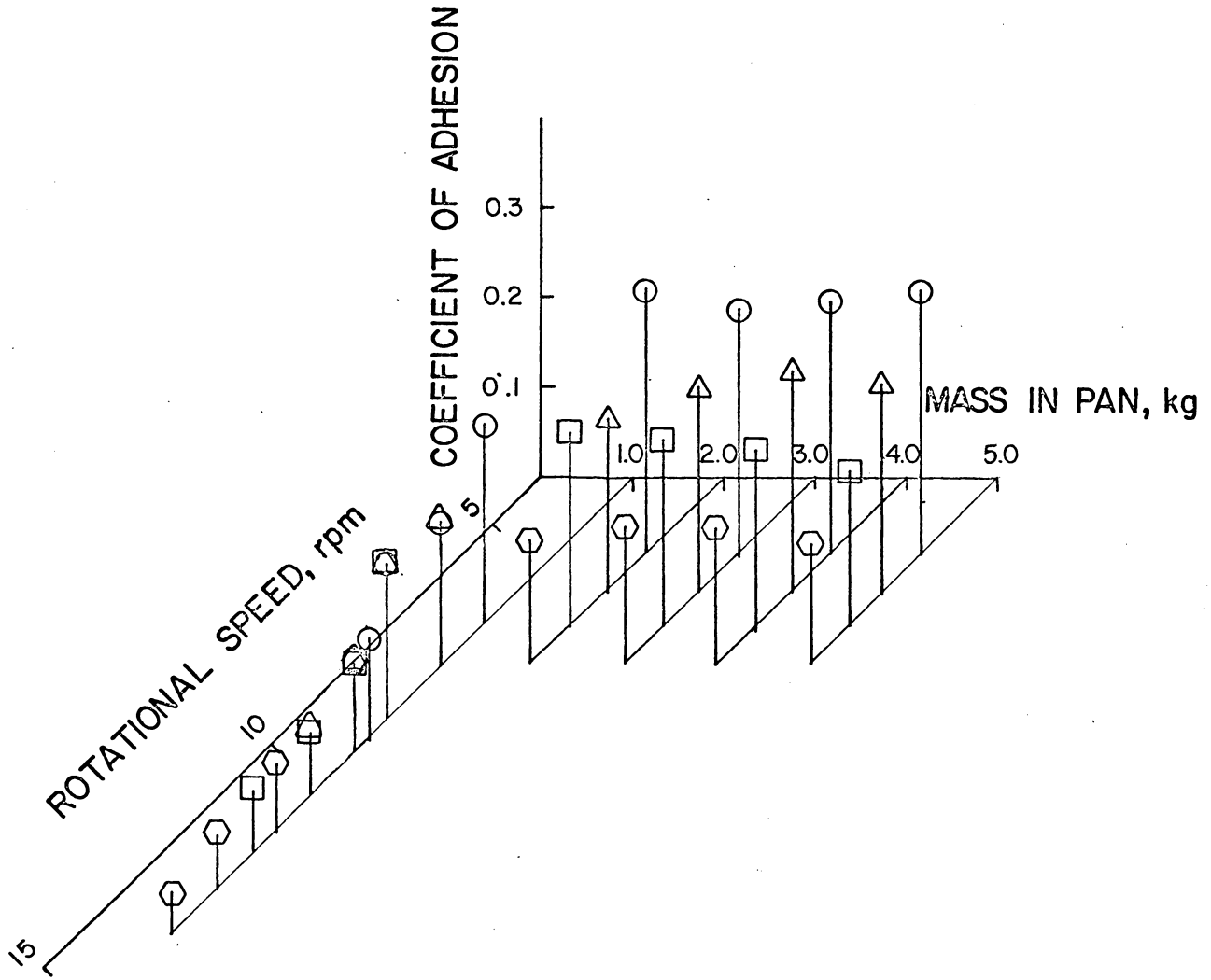

Fig. 16. Coefficient of adhesion values against rotational speed and mass in load pan

and 8310 revolutions per minute of the small wheel. The calculations for the velocity into the contact area are shown in Appendix 9.2. The plots are shown in Fig. 17, 18, 19 and 20 respectively for the four base speeds of 5770, 6490, 7270 and 8310 revolutions per minute of the small wheel. A graph of the variation of the coefficient of adhesion with contact velocity regardless of the speed of rotation of the small wheel was also drawn and is shown in Fig. 21.

A cursory glance at Fig. 21 indicates a drop in the coefficient of adhesion for increasing contact velocity for the four base speeds at which the tests were conducted.* However on grouping the various data points which were obtained from fixed speeds of rotation of the small wheel it is evident that the drop in the coefficient of adhesion for increasing contact velocity is due to a change in the rotational speed level of the small wheel and is not related to the normal load. Again a study of Fig. 17, 18, 19 and 20 indicates the possibility of two coefficients of adhesion for a fixed contact velocity which is very improbable. As a result it is doubtful whether contact velocity is an operating variable of the coefficient of adhesion. (*Shown by the broken line on Fig. 21)

5.3 Effect of Dwell Time on the Coefficient of Adhesion

Figure 22 shows a plot of the dwell time in the contact ellipse against the coefficient of adhesion. In the plot, data points for which the speed of rotation of the small wheel was kept constant

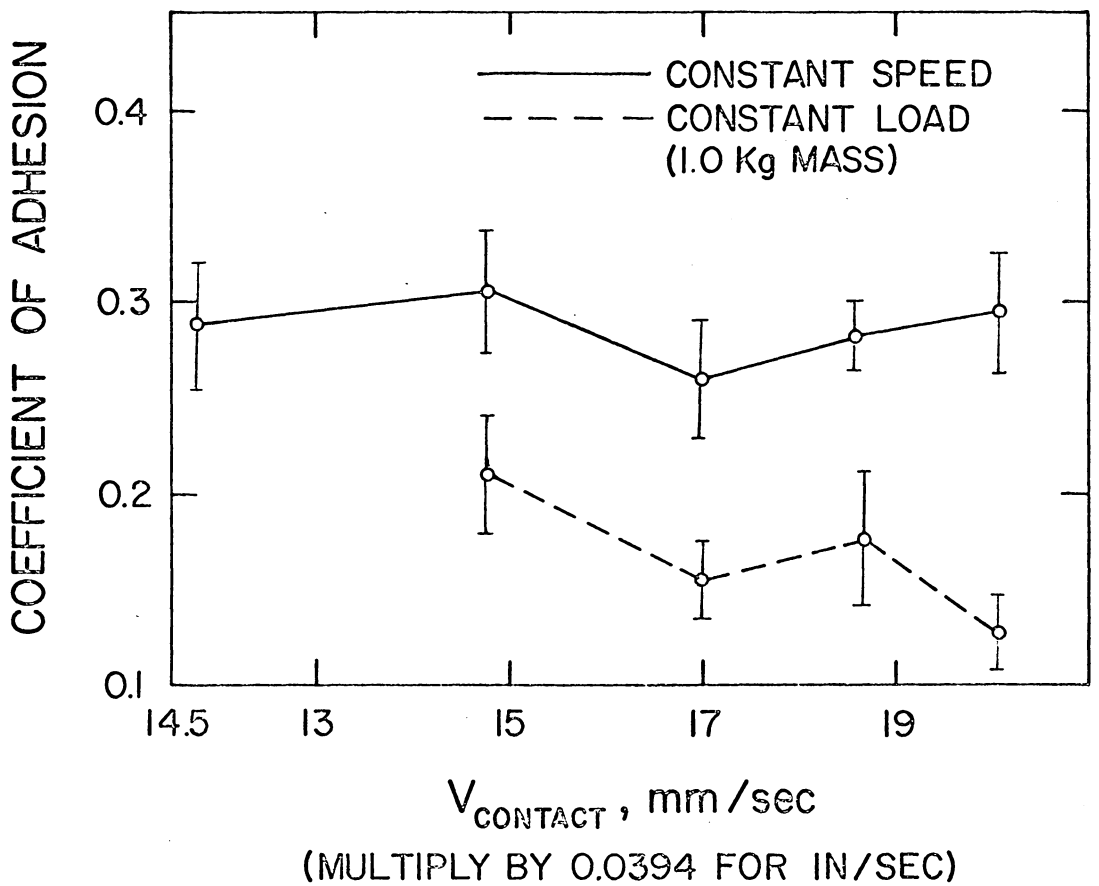

Fig. 17. Coefficient of adhesion-contact velocity curve for a rotational speed of 5770 rpm of the small wheel shown with 95% confidence limit.

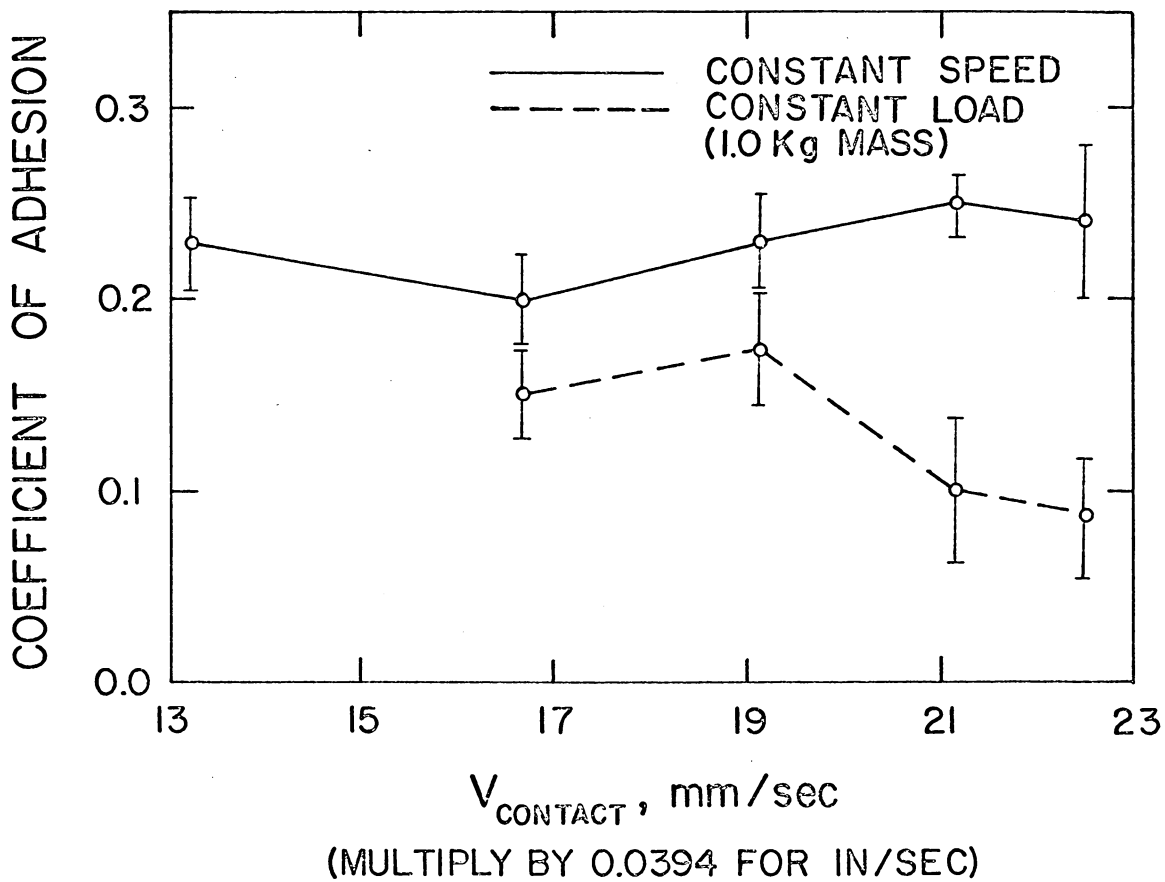

Fig. 18. Coefficient of adhesion-contact velocity curve for a rotational speed of 6490 rpm of the small wheel shown with 95% confidence limit

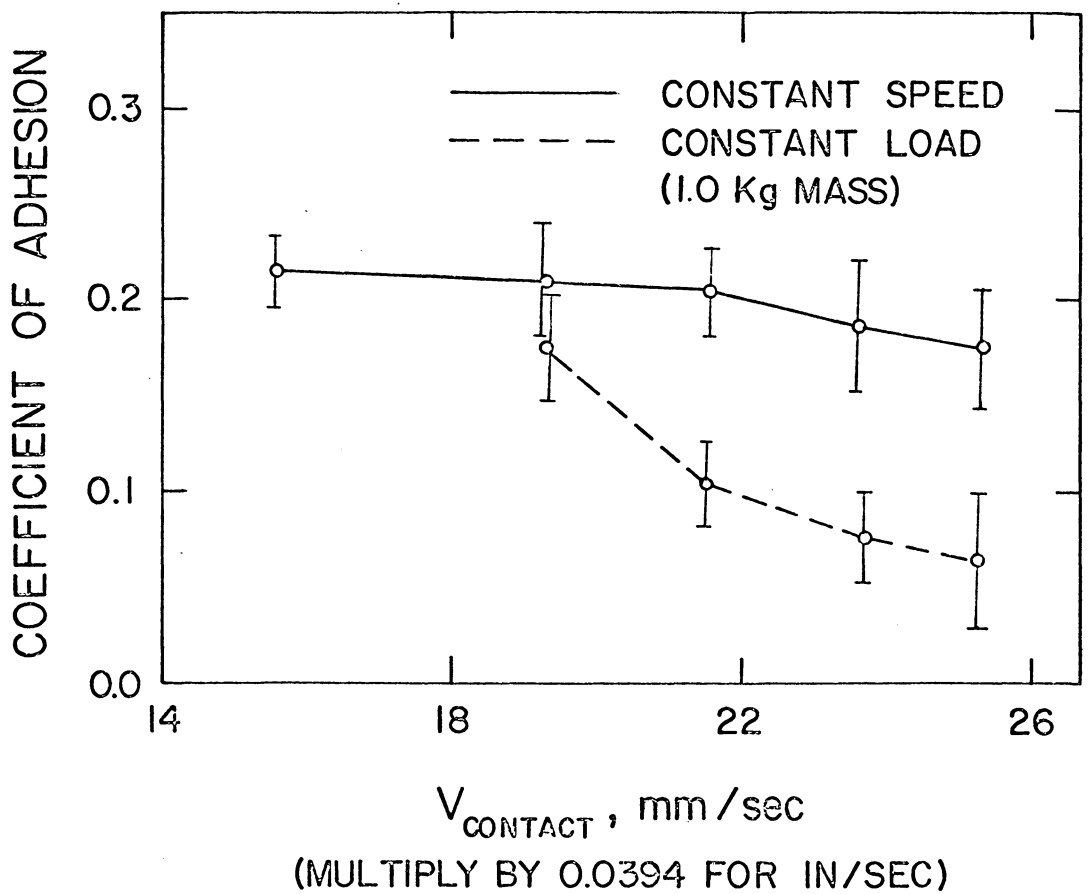

Fig. 19. Coefficient of adhesion-contact velocity curve for a rotational speed of 7270 rpm of the small wheel shown with 95% confidence limit

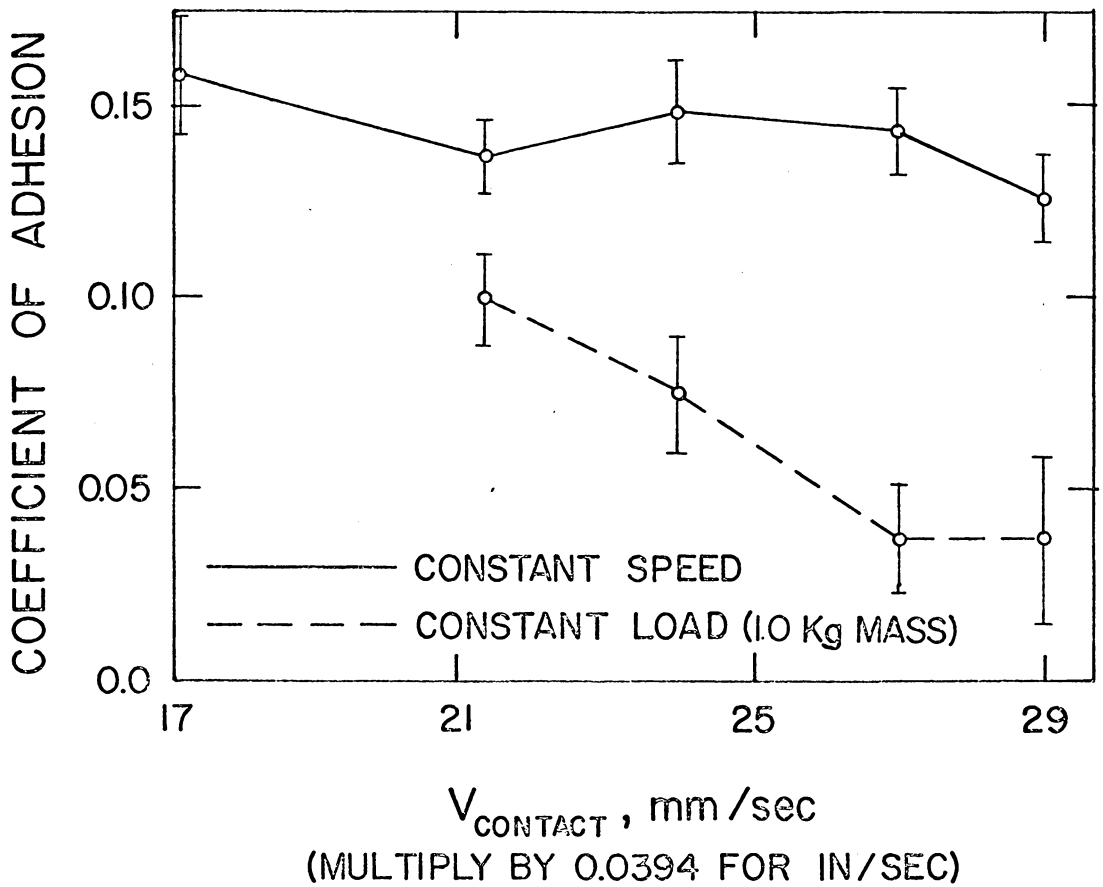

Fig. 20. Coefficient of adhesion-contact velocity curve for a rotational speed of 8310 rpm of the small wheel shown with 95% confidence limit

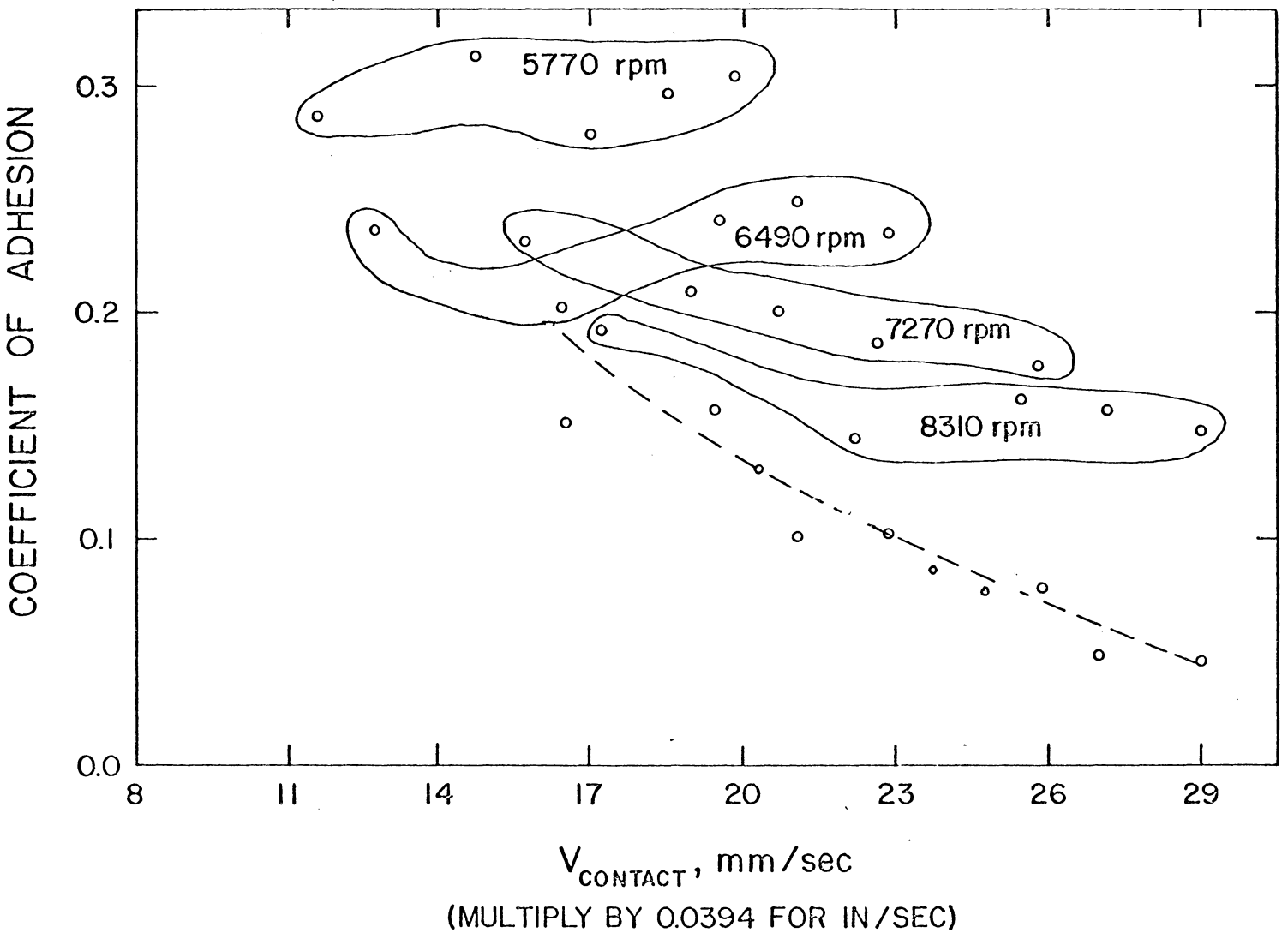

Fig. 21. Coefficient of adhesion values against contact velocity

and the normal load increased are grouped together by circling the points with a freehand curve.

An inspection of Fig. 22 indicates that the data points enclosed by the free hand curves have no bearing on the trend of the plot which shows an increase in the coefficient of adhesion with an increase in the dwell time in the contact ellipse. This observation confirms the doubts raised in the previous section about the validity of contact velocity as an operating variable of the coefficient of adhesion.

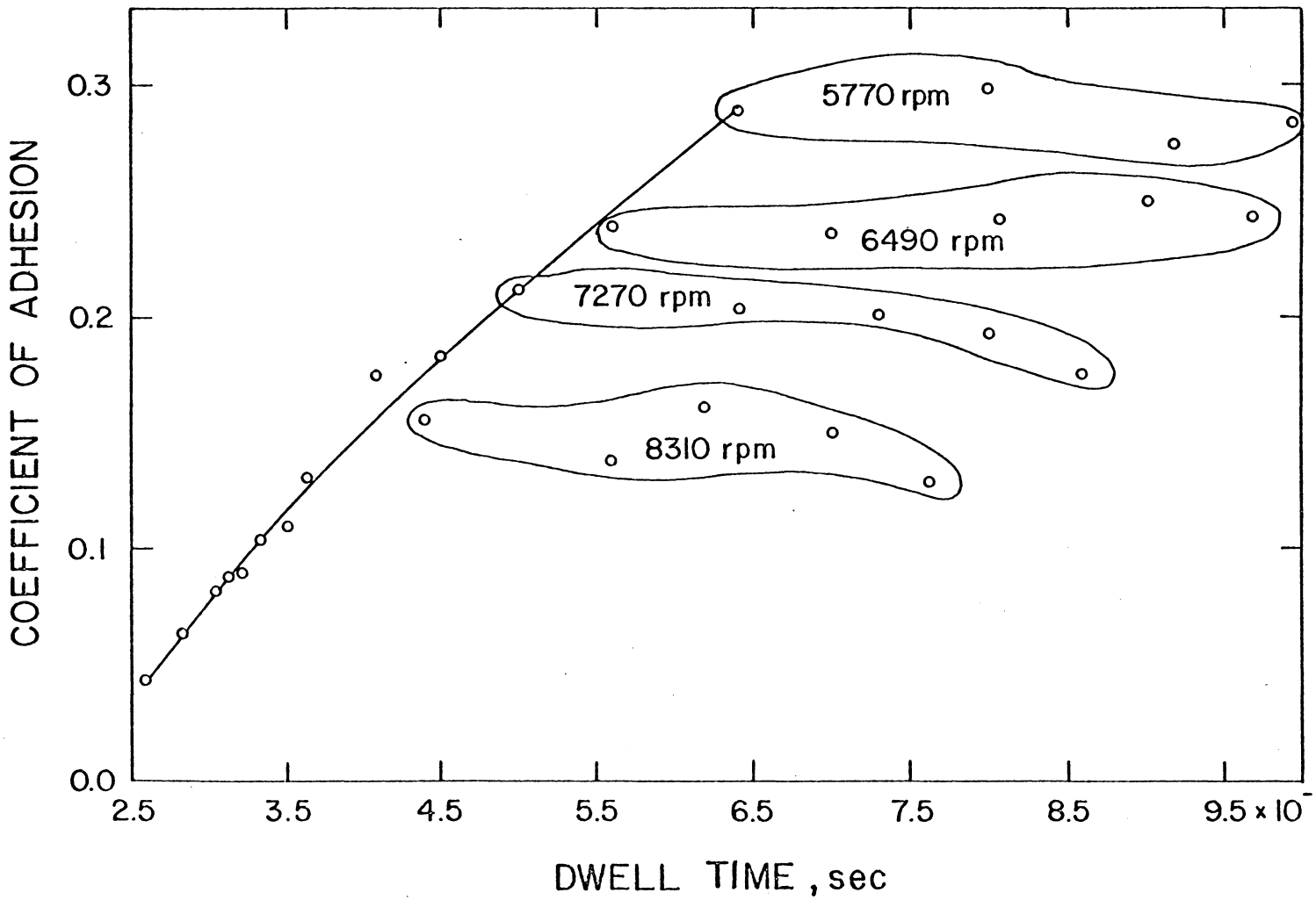

Fig. 22. Coefficient of adhesion values against dwell time

6. CONCLUSIONS

1. The test results show that contact velocity and dwell time (which accounts for an increase in the width of the contact ellipse) are not among the operating variables affecting the coefficient of adhesion in rolling contact. This conclusion is contrary to that of M. E. Anderson (8), who suggested that the decrease in the coefficient of adhesion with increasing speed was due to a decrease in the adhesion strength of the asperity junctions because of the decrease of time in the contact area.

2. The independence of the coefficient of adhesion from the normal load has been verified and corroborates most of the previous rolling adhesion studies.

3. The decrease in the coefficient of adhesion with increasing speed has been verified.

7. RECOMMENDATIONS

1. Effects of surface vibration on the coefficient of adhesion. Possible tests could be:

   a) Increasing the surface vibration for a fixed rotational speed.

   b) Increasing the surface speed for a fixed level of surface vibration.

Thus, using the frictional oscillations model viz. a spring and damper, the equivalent stiffness of the shaft could be evaluated and used as a spring model in the actual experimentation.

2. Effects of surface contaminants viz. the study of the coefficient of adhesion on:

   a) Lubricated surfaces.

   b) Dry surfaces.

3. Effects of surface roughness and longitudinal creep on the coefficient of adhesion.

8. REFERENCES

1. Kendall, K., "Rolling Friction and Adhesion Between Smooth Solids", Wear, Vol. 33, 1975, pp. 351-358.
2. Greenwood, N. A., and D. Tabor, "The Friction of Hard Sliders on Lubricated Rubber. The Importance of Deformation Losses", Proceedings of the Physics Society, Vol. 71, 1958, pp. 989-1001.
3. Tabor, D., "The Mechanism of Free Rolling Friction", Lubrication Engineering, Vol. 12, 1956, pp. 379-386.
4. Johnson, K. L., "Tangential Tractions and Micro-slip in Rolling Contact", Rolling Contact Phenomena, J. B. Bidwell (Editor), Elsevier, Amsterdam, Netherlands, 1960.
5. Andrews, H. J., "The Contact Between a Locomotive Driving Wheel and the Rail", Wear, Vol. 178, Part 3E, 1964, pp. 145-158.
6. Hewko, L. O., F. G. Rounds, and R. L. Scott, "Tractive Capacity and Efficiency of Rolling Contacts", Proceedings of the Symposium on Rolling Contact Phenomena, Elsevier, Amsterdam, Netherlands, 1962, pp. 157-185.
7. Koffman, J., "Adhesion and Friction in Rail Traction", Journal of the Institution of Locomotive Engineers, Vol. 38, 1948, pp. 593-641.
8. Anderson, M. E., A Study of Rolling Adhesion by Simulating Wheel/Rail Interaction, M. S. Thesis, Virginia Polytechnic Institute and State University, Blacksburg, Virginia, Sept. 1977.

9. Kirk, W. B., "High Speed Train Operation", Proceedings of the Winter Meeting of the ASME, Chicago, Illinois, November 1965.

10. Burwell, J. T., and E. Rabinowicz, "The Nature of the Coefficient of Friction", Journal of Applied Physics, Vol. 24, Number 2, pp. 136-139.

11. Timoshenko, S., Strength of Materials, Part II, Advanced Theory and Problems, Robert E. Krieger Publishing Company, Inc., New York, 1976, pp. 339-345.

12. Rabinowicz, E., Friction and Wear of Materials, John Wiley and Sons, Inc., New York, 1965, pp. 83-85.

9. APPENDICES

9.1 Calculation of Semi-Major and Semi-Minor Axis of the Ellipse of Contact.

9.2 Calculation of Velocity into the Contact Area

9.3 Calculation of Dwell Time in the Contact Ellipse

9.4 Equipment

9.1 Calculation of Semi-Major and Semi-Minor Axis of Ellipse of Contact

The calculation of the semi-major and semi-minor axis of the ellipse of contact is based on Hertz's equations as explained by S. Timoshenko (11).

For the case of two elastic bodies in contact in the direction of the normal to the tangent plane, the surface of contact is an ellipse.

The magnitudes of the semiaxes of the contact ellipse are given by the equations

$$a = m \sqrt[3]{\frac{3\pi N}{A} \frac{(K_1 + K_2)}{A + B}} \tag{1}$$

$$b = n \sqrt[3]{\frac{3\pi N}{A} \frac{(K_1 + K_2)}{A + B}} \tag{2}$$

where m, n are values obtained from Table 9 for θ defined by

$$\text{Cos } \theta = \frac{B - A}{A + B} \tag{3}$$

The constants A and B are obtained from the equations

$$A + B = \frac{1}{2} \left(\frac{1}{R_1} + \frac{1}{R_1'} + \frac{1}{R_2} + \frac{1}{R_2'} \right) \tag{4}$$

$$B - A = \frac{1}{2} \left\{ \left(\frac{1}{R_1} - \frac{1}{R_1'} \right)^2 + \left(\frac{1}{R_2} - \frac{1}{R_2'} \right)^2 + 2 \left(\frac{1}{R_1} - \frac{1}{R_1'} \right) \left(\frac{1}{R_2} - \frac{1}{R_2'} \right) \text{Cos } (2\psi) \right\}^{\frac{1}{2}} \tag{5}$$

Table 9. The values of m and n for various values of θ as calculated by S. Timoshenko (11)

θ	m	n
30	2.731	0.493
35	2.397	0.530
40	2.136	0.567
45	1.926	0.604
50	1.754	0.641
55	1.611	0.678
60	1.486	0.717
65	1.378	0.759
70	1.284	0.802
75	1.202	0.846
80	1.128	0.893
85	1.061	0.944
90	1.000	1.000

where R_1 and R_1' represent the principle radii of curvature at the point of contact of one of the bodies and R_2 and R_2' those of the other and 4 the angle between the normal planes containing the curvatures $\frac{1}{R_1}$ and $\frac{1}{R_2}$.

K_1 and K_2 are defined by equation

$$K_{1,2} = \frac{1 - \gamma_{1,2}^2}{\pi E_{1,2}} \qquad (6)$$

where $\gamma_{1,2}$ is the Poisson's ratio of the material and $E_{1,2}$ is the modulus of elasticity.

A summary of the calculations for the major and minor semi-axis of the contact ellipse, for the loads used in the tests follows

(1) For steel: $\gamma = 0.3$

$E = 207 \times 10^3$ MPa $\qquad (30.0 \times 10^6$ p.s.i.)

$$K_1 = K_2 = \frac{1 - \gamma^2}{\pi E}$$

$$= \frac{1 - 0.3^2}{\pi \times 207 \times 10^9}$$

$$= 1.4 \times 10^{-12} \quad m^2/N$$

(2) For the large wheel (body 1) $R_1 = 11.5$

$R_1' = \alpha$

For the small wheel (body 2) $R_2 = 1$

$R_2' = 2$

$\psi = 90^o$

$$\therefore A + B = \frac{1}{2}\left(\frac{1}{R_1} + \frac{1}{R_1'} + \frac{1}{R_2} + \frac{1}{R_2'}\right)$$

$$= \frac{1}{2}\left(\frac{1}{11.5} + \frac{1}{\alpha} + \frac{1}{1} + \frac{1}{2}\right)$$

$$= 0.7935$$

$$B - A = \frac{1}{2}\left\{\left(\frac{1}{R_1} - \frac{1}{R_1'}\right)^2 + \left(\frac{1}{R_2} - \frac{1}{R_2'}\right)^2 + 2\left(\frac{1}{R_1} - \frac{1}{R_1'}\right)\left(\frac{1}{R_2} - \frac{1}{R_2'}\right)\text{Cos}(2\psi)\right\}^{1/2}$$

$$= \frac{1}{2}\left\{\left(\frac{1}{11.5} - \frac{1}{\alpha}\right)^2 + \left(\frac{1}{1} - \frac{1}{2}\right)^2 + 2\left(\frac{1}{11.5} - \frac{1}{\alpha}\right)\left(\frac{1}{1} - \frac{1}{2}\right)\text{Cos}(180^o)\right\}^{1/2}$$

$$= 0.2065$$

(3) $$\text{Cos}\ \theta = \frac{B - A}{A + B}$$

$$= \frac{0.2065}{0.7935}$$

$$= 0.2602$$

$$\theta = 74.9^o$$

From Table 9, m - 1.130 and n - 0.89

(A) $$a = m\sqrt{\frac{3\pi N}{A}\ \frac{(K_1 + K_2)}{A + B}}$$

$$= 1.13\ \sqrt[3]{\frac{3\pi N}{4}\ \frac{2 \times 1.4 \times 10^{-12}}{0.7935}}\ m$$

$$= 2.2892 \times 10^{-2} \times \sqrt[3]{N}\ cm$$

$$b = n\ \sqrt[3]{\frac{3\pi N}{A}\ \frac{(K_1 + K_2)}{A + B}}$$

$$= 0.89\ \sqrt[3]{\frac{3\pi N}{A} \times \frac{2 \times 1.4 \times 10^{-12}}{A + B}}\ m$$

$$= 1.803 \times 10^{-2} \times \sqrt[3]{N}\ cm$$

The values for the semi-major and semi-minor axis of the ellipse of contact for the different loads used in the tests are tabulated in Table 10.

Table 10. Calculated values of semi-major axis (a) and semi-minor axis (b) of the contact ellipse for different masses in the load pan.

Mass in load pan (kg)	Semi-major axis a (cm)	Semi-minor axis b (cm)
1	0.0980	0.0771
2	0.1235	0.0970
3	0.1414	0.1113
4	0.1555	0.1225
5	0.1676	0.1319

9.2 Calculation of Velocity into the Contact Area

The velocity into the contact area is equal to the magnitude of the smaller semi axis of the ellipse of contact times the angular velocity i.e.

$$v_{\text{contact area}} = b \times \omega$$

But from equation 2,

$$b = n \sqrt[3]{\frac{3\pi N}{4} \frac{(K_1 + K_2)}{A + B}}$$

$$\therefore \quad v_{\text{contact area}} \propto \sqrt[3]{N} \quad \text{, for constant } \omega$$

Thus if N is increased to 2N, 3N, 4N, 5N, $v_{\text{contact area}}$ increases by 26%, 44%, 59% and 71%.

Thus to verify the interdependence of load and velocity into the contact area, it was required to find the coefficient of adhesion at a fixed speed and various loads (in steps of 1kg) and subsequently to increase the speed in steps of 26%, 44%, 59%, 71%.

The four base speeds selected were 5770, 6490, 7270 and 8310 rpm. of the small wheel.

The $v_{\text{contact area}}$ for the different speeds and loads for which the tests were conducted is shown in Table 11.

Table 11. Calculated values of the $v_{\text{contact area}}$ for the different loads land speeds for which the tests were conducted.

	Number of masses in load pan				
	1	2	3	4	5
Rotational Speed of small wheel, rpm	$v_{\text{contact area}}$, cm/sec.				
5770	1.1803	1.4849	1.7038	1.8752	1.0191
6490	1.3279	1.6706	1.9169	2.1098	2.2717
7270	1.4872	1.8711	2.1469	2.3630	2.5443
8310	1.6990	2.1384	2.4537	2.7006	2.9078
8180	1.6731				
9310	1.9122				
9870	2.0184				
10350	2.1113				
11100	2.2706				
11560	2.3645				
11960	2.4470				
12430	2.5421				
13215	2.7023				
14210	2.9065				

9.3 Calculation of Dwell Time in the Contact Ellipse

The calculations for the dwell time in the contact ellipse are based on the deformations of the small wheel/large wheel in the area of contact.

From Fig. 23 we have,

$$\text{Sin } \theta_1 = \frac{\ell}{R_1} = \frac{V_{A1}}{R_1 \omega_1}$$

$$\therefore V_{A1} = \ell\omega_1$$

and $$V_{A2} = \ell\omega_2$$

$$\therefore V_A = V_{A1} + V_{A2} = \ell(\omega_1 + \omega_2)$$

Also $$t = \frac{2\ell}{R_1'\omega_1}$$

But $$R_1' = R_1 \text{ Cos } (\theta_1)$$

$$\therefore t = \frac{2\ell}{R_1\omega_1 \text{ Cos}(\theta_1)} \qquad (7)$$

The values of the dwell time for the different loads and speeds for which the tests were conducted are tabulated in Table 12.

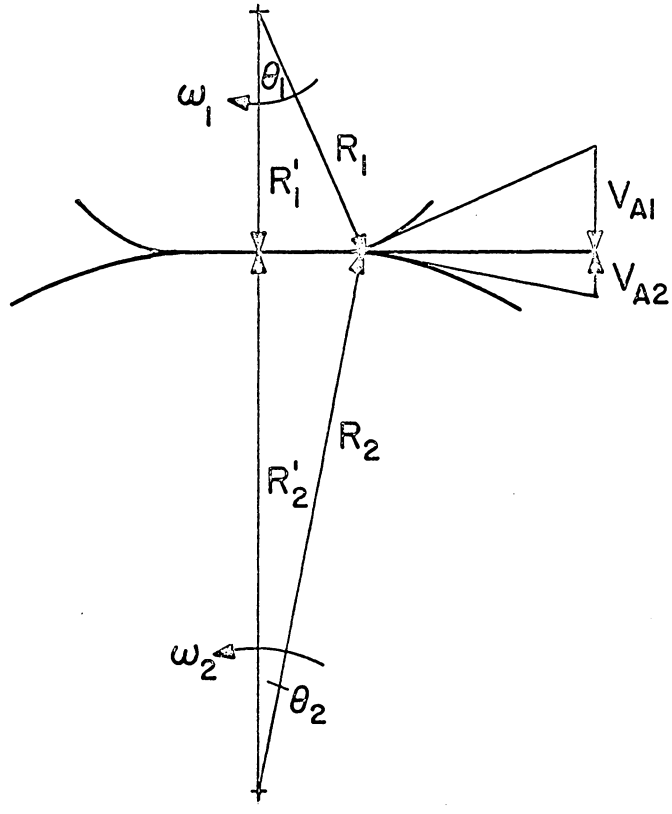

Fig. 23. Deformation of small/large wheel in the contact zone

Table 12. Calculated values of the dwell time for the different loads and speeds for which the tests were conducted.

	Number of masses in load pan				
	1	2	3	4	5
Rotational Speed of small wheel, rpm	Dwell time, sec. x 10^{-5}				
5770	6.3869	8.0480	9.2153	10.1351	10.9245
6490	5.6772	7.1551	8.1929	9.0105	9.7124
7270	5.0685	6.3868	7.3131	8.0355	8.6695
8310	4.4348	5.5883	6.3988	7.0375	7.5857
8180	4.5053				
9310	3.9320				
9870	3.7347				
10350	3.5714				
11100	3.3197				
11560	3.1881				
11960	3.0805				
12430	2.9653				
13215	2.7895				
14210	2.5935				

9.4 Equipment

The following is a list of equipment used in conjunction with the test rig.

Quantity	Description	Serial No.
1	Hewlett Packard 5233L Frequency Counter	529-01830
1	Hewlett Packard 5326A Frequency Counter	1116A0075A
1	Breul and Kjaer Strain Gage Apparatus Type 1516	132912
2	Gould Brush 220 Strip Chart Recorders	12099 and 04986
2	Magnetic Transducers Electro 3045A	
	Miscellaneous: Resistance-capacitance filters, diodes, resistors, capacitors, cables.	

The vita has been removed from the scanned document

A STUDY OF ROLLING ADHESION IN BRAKING

by

John Roy D'Sa

(ABSTRACT)

The effect of normal load, contact velocity, and dwell time on the coefficient of adhesion at slip in braking was investigated. A test rig that simulated locomotive wheel/rail interactions was used for the experimentation.

The results indicated a drop in the coefficient of adhesion with increasing speed. However, normal load, contact velocity, and dwell time, as operating variables, did not have any effect on the variation of the coefficient of adhesion.

A description of the investigation and recommendations for further studies is included.